

Star formation within globular clusters: discrete multiple bursts and top-light mass functions

Kenji Bekki^{1*}

¹*ICRAR M468 The University of Western Australia 35 Stirling Hwy, Crawley Western Australia 6009, Australia*

Accepted, Received 2005 February 20; in original form

ABSTRACT

The observed discrete multiple stellar populations and internal abundance spreads in r - and s -process elements within globular clusters (GCs) have been suggested to be explained self-consistently by discrete star formation events over a longer timescale ($\sim 10^8$ yr). We here investigate whether such star formation is really possible within GCs using numerical simulations that include effects of dynamical interaction between individual stars and the accumulated gas (“star-gas interaction”) on star formation. The principal results are as follows. Small gas clouds with densities larger than 10^{10} atoms cm^{-3} corresponding to first stellar cores can be developed from gas without turbulence. Consequently, new stars can be formed from the gas with high star formation efficiencies (> 0.5) in a bursty manner. However, star formation can be suppressed when the gas mass fractions within GCs (f_g) are less than a threshold value ($f_{g,\text{th}}$). This $f_{g,\text{th}}$ is larger for GCs with lower masses and larger gas disks. Star-gas interaction and gravitational potentials of GCs can combine to suppress the formation of massive stars (i.e., “top-light” stellar initial mass function). Formation of He-rich stars directly from gas of massive AGB stars is possible in massive GCs due to low $f_{g,\text{th}}$ (< 0.01). Short bursty star formation only for $f_g > f_{g,\text{th}}$ can be partly responsible for discrete multiple star formation events within GCs. We discuss how these results depend on the adopted model assumptions, such as rotating gas disks within GCs.

Key words: ISM: dust, extinction – galaxies:ISM – galaxies:evolution – infrared:galaxies – stars:formation

1 INTRODUCTION

It is one of crucial questions in observational and theoretical studies of globular clusters (GCs) why the Galactic GCs are observed to show internal abundance spreads in various elements to different degrees (Gratton et al. 2012 for a review). The vast majority of GCs clearly show internal abundance spreads only in light elements (e.g., Carretta et al. 2009), however, some Galactic GCs have been observed to show such spreads even in $[\text{Fe}/\text{H}]$ (e.g., Da Costa et al. 2009; Marino et al. 2009, 2011, 2018; Johnson et al. 2015; Yong et al. 2014). These “Fe-anomalous” GCs also show internal abundance spreads in s -process elements (e.g., Marino et al. 2011; Yong et al. 2014; Lardo et al. 2013), though Carretta et al. (2015) have found internal spreads in s -process elements (e.g., La) in M80, which is not classified as a Fe-anomalous GC. Furthermore, internal abundance spreads have been found in helium for some GCs (e.g., Piotto et

al. 2005; Milone et al. 2017) and in r -process elements for 6 GCs (e.g., Snedden et al. 1997; Roederer 2011).

It is one of goals for theoretical studies of GC formation to construct a model that explains self-consistently (i) the origin of the almost universal anti-correlations between light elements (Na-O and Mg-Al) and (ii) internal abundance spreads in r - and s -process elements and iron observed in a significant fraction of the Galactic GCs. One of popular scenarios for the formation of GCs with multiple stellar populations (MSPs) is that second generations (“2G”) of stars were formed from gas ejected from first generations (“1G”) in the early formation histories of GCs. The chemical abundances of 2G stars depend on various factors, such as whether the gas from 1G stars was mixed with pristine gas or not. These self-enrichment processes have been now investigated by many theoretical models of GC formation.

Various scenarios have been proposed so far to explain the observed properties of GCs with MSPs (e.g., Renzini et al. 2015; Bastian & Lardo 2018 for recent reviews). Recent observational studies of internal abundance spreads in r -process elements (e.g., Roederer 2011; Sobeck et al. 2011;

* E-mail: kenji.bekki@uwa.edu.au

Table 1. Possible positive and negative effects of existing (1G) stars within GCs on the formation of later generations (LG; 2G, 3G etc) of stars from gas accumulated within GCs.

Physical process	Possible effects	Reference
Global potentials of GCs	Retention of gas ejected from stars	D08, B11
Capture of cold gas	Gas fueling for star formation	BM09, PK09
Heating by compact objects	Expulsion of cold gas from GCs	L13
Radiative feedback effects of young 1G stars	Heating and evaporation of cold gas	CS11
Thermal and kinetic feedback of AGB stars	Removal of gas from GCs	D08, B11, B17b
Type Ia SN from 1G stars	Heating and expulsion of gas	D08, D16
Type II SN from multiple generations of stars	Heating and expulsion of gas	BJK17, B18
Delayed SNII	Rapid removal of AGB ejecta	D16, DDV16
Collisions of 1G stars with PMS stars	Disruption of accretion disks	T15
Direct stellar bombardment (SB) on gas clouds	Tidal perturbation to growing gas clouds	This work

Worley et al. 2013) have been suggested to provide very strong constraints on the theoretical models of GCs: formation scenarios in which self-enrichment can occur before merging between neutron stars (earlier than 10^7 yr after 1G star formation) could be possibly ruled out (e.g., Bekki & Tsujimoto 2017, BT17). Furthermore, the observed discrete subpopulations of GCs (e.g., Caretta 2014; Carretta et al. 2018) can be explained by discrete epochs of star formation from AGB ejecta mixed with pristine gas (e.g., Bekki et al. 2017, BJP17). Top-light initial mass functions (IMFs) of stars in intra-cluster medium (ICM) with lower densities can be responsible for the prolonged star formation within GCs in BJP17, though such IMF variations are still being discussed extensively (e.g., Kroupa et al. 2013 for detailed discussion on this issue). Kim & Lee (2018) have recently proposed that star formation from AGB ejecta mixed with stellar winds of massive stars and gas left from original star-forming molecular clouds is responsible for the origin of discrete MSPs within GCs.

D’Antona et al. (2016, D16) have proposed a GC formation scenario in which Fe-rich ejecta from SNIa or delayed SNII can be mixed with AGB ejecta to form 2G (and 3G) stars with their Fe abundances being slightly higher than those of 1G stars. In their scenario, delayed SNII can truncate star formation from AGB ejecta: influences of SNII from 2G are, however, completely ignored. These recent works have demonstrated that the AGB scenario can be the most promising candidate that can explain anti-correlations between abundances of light elements, discrete populations, and internal abundance spread in various elements (e.g., *s*-process) within GCs. However, it is fair to say that it is yet to be determined which scenario is the most realistic and reasonable one, mainly because the details of relevant physical processes in each scenario, in particular, secondary star formation in gas from 1G stars, have not been extensively investigated.

One of possibly important physical processes related to star formation in GCs is dynamical interaction between individual GC stars and collapsing star-forming gaseous clouds within GCs. Owing to the very high number density of stars in a GC ($> 10^4$ stars pc^{-3}), direct encounters of stars with gravitationally collapsing gas clouds can influence the growth processes of such clouds: this situation is dramatically different from star formation in isolated fractal molecular clouds with no existing stars, which have been investigated by many authors (e.g., Klessen et al. 1998; Dale et al. 2011). It would be possible that such star-cloud interaction tidally disturbs the surrounding regions of collapsing gas

clouds and consequently suppress the growth of the clouds. Cumulative effects of numerous star-cloud interaction (referred to as “stellar bombardment”, SB) could have some dramatic effects on the evolution of gas accumulated into GCs under some circumstances. Previous numerical simulations could not investigate this possibly important physical process, because they could not resolve the gas density of 10^{10} atom cm^{-3} corresponding to the typical density of first stellar core (e.g., Meyers 1978; Saigo et al. 2000) owing to the relatively poor numerical resolutions: B11 investigated secondary star formation on a scale of 1 – 10 pc, therefore it could not resolve the scale of first stellar cores.

The purpose of this paper is thus to investigate, for the first time, how SB can influence the growth of gas clumps for star formation in GCs. We particularly investigate whether and how gas clouds with densities more than 10^{10} atoms cm^{-3} corresponding to typical densities of first stellar cores (e.g., Myers 1978; Saigo et al. 2001) using our original hydrodynamical simulations of gas evolution in such dense systems. We also investigate how the results depend on (i) the original masses and sizes of GCs and (ii) the gas mass fractions (f_g) in GCs in order to understand under what physical conditions secondary star formation is possible. This investigation can reveal the details of secondary star formation processes and thus provide valuable insights for the origin of MSPs in GCs. Since this is the very first investigation on this important issue, we do not include chemical evolution of gas during secondary star formation within GCs. We also adopt a dynamical equilibrium model for all GC simulations, which means that more realistic growth processes of cluster formation through hierarchical merging of subclusters or cluster complex (e.g., Adamo et al. 2012; Bekki 2017a, B17a) are totally ignored.

The SB effects on star formation can be only one of several key effects of stars on star formation within GCs. Positive and negative effects of existing stars of GCs on secondary star formation have been discussed in previous studies and are briefly summarized in Table 1 for comparison. These include (1) retention of gas due to global gravitational potentials of GCs (e.g., D’Ercole et al. 2008, D08; Bekki 2011, B11), (2) gravitational capture of cold gas by GCs (e.g., Bekki & Mackey 2009, BM09; Pflamm-Altenburg & Kroupa 2009, PK09, Armstrong et al. 2018), (3) heating of ICM by compact objects such as stellar mass black holes (e.g., Leigh et al. 2013, L13), (4) radiative feedback effects of young stars (Conroy & Spergel 2010, CS11), (5) feedback effects of AGB stars (D08; B11; Bekki 2017b, B17b), (6) SNIa explosions (D08, D16), (7), SNII explosions from

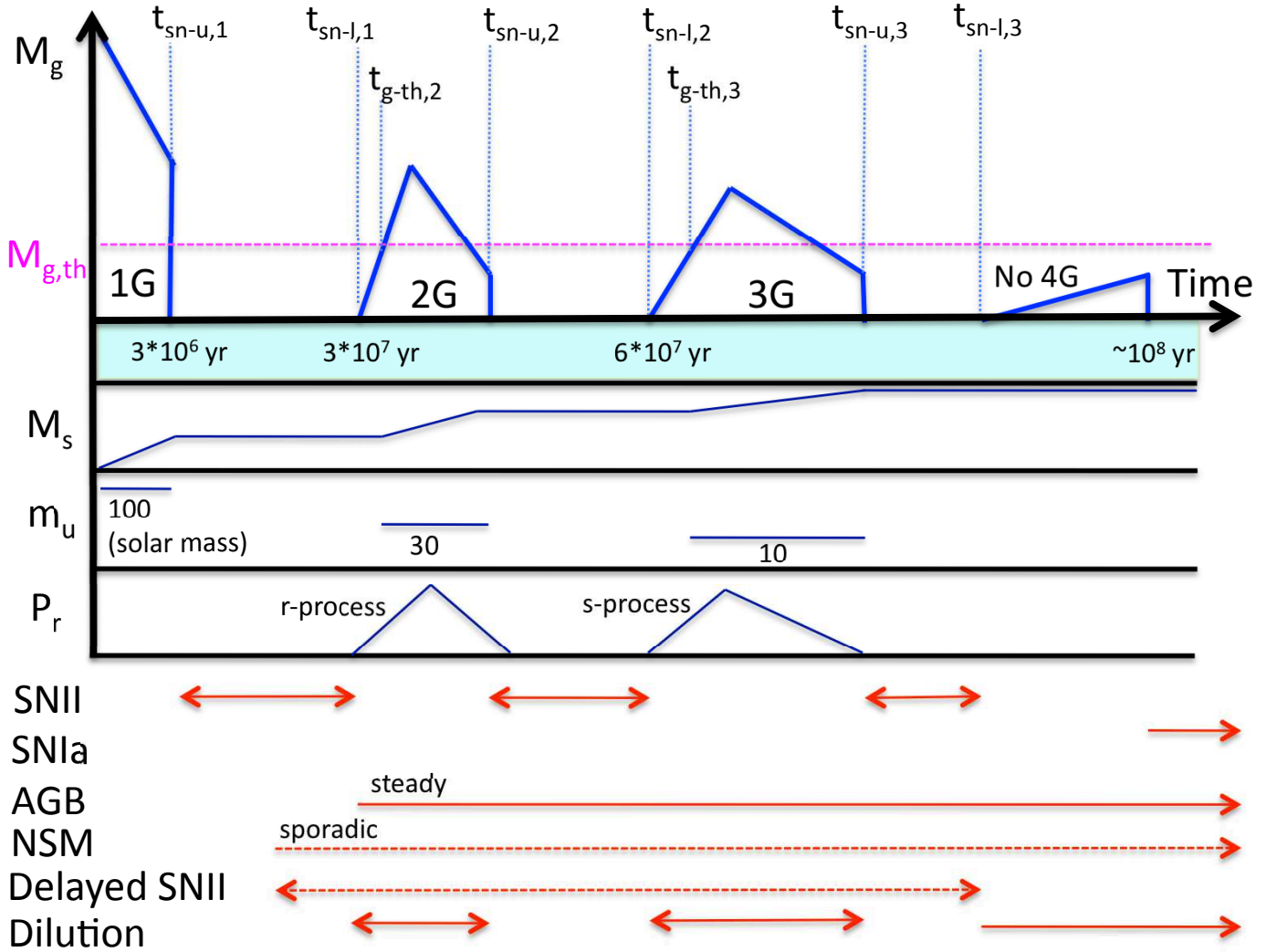


Figure 1. Illustration of the AGB scenario for the origins of discrete multiple stellar populations (e.g., 1G means the first generation of stars) and internal abundance spreads for various elements (e.g., s - and r -process). Time evolution of the total gas mass (M_g), the total mass of new stars formed from gas (M_s), the upper-mass cut-off of the IMF (m_u), and the retention probability of gas that is consumed by secondary star formation (P_r) is shown. Red arrows indicate duration when each object (e.g., SNII) greatly influences and chemically pollutes ICM. Gas ejection from AGB stars can steadily continue due to contribution from the stars with different masses whereas gas ejection from neutron star merging (NSM) can occur sporadically. Delayed core-collapse supernovae from binary massive stars could occur sporadically too until 200 Myr after the formation of 1G stars (e.g., Zapartas et al. 2017). Multiple epochs when dilution of AGB ejecta by pristine gas can be efficient are also shown by red arrows. The epochs of the most and least massive SNII from i -th generation of stars are indicated by $t_{sn-u,i}$ and $t_{sn-l,i}$ respectively (here $i=1, 2$, and 3 only). Also the time when M_g exceeds the threshold gas mass/fraction for star formation ($M_{g,th}$) is indicated for each discrete star formation event (e.g., $t_{g-th,2}$ for 2G formation). Star formation can be truncated either if SNe can expel the gas left from star formation (for $m_u \geq 8M_\odot$) or if M_g or f_g (gas mass fraction) becomes less than $M_{g,th}$ or $f_{g,th}$ (for $m_u < 8M_\odot$). A crucial parameter in this figure is the threshold gas mass ($M_{g,th}$) or mass fraction ($f_{g,th}$) above which star formation from non-turbulent gas is possible within GCs. Since gas ejection from AGB stars steadily continues, secondary star formation from the gas is expected to continue steadily too. However, in this scenario, $M_{g,th}$ and SNII does not allow such continuous star formation under some circumstances (e.g., $m_u \geq 8M_\odot$).

multiple generations of stars (BJK17; Balin 2018, B18), (8) disruption of accretion disks around pre-main-sequence stars (PMS) by collisions of 1G stars (Tailo et al. 2015, T15), and (9) delayed SNII (D16, D’Ercole et al., 2016, DDV16).

For & Bekki (2017) have recently discovered young stellar objects (YSOs) in younger star clusters in the LMC, which is evidence that gas exists within the clusters (or it existed until quite recently). This new observation can justify the adopted assumption of cold gas within star clusters, though no observations have ever revealed H α emission from

massive OB stars within star clusters in star-forming galaxies. The observed lack of OB stars in young clusters is not necessarily inconsistent with secondary star formation, because the upper-mass cut-off (m_u) of the IMF can be less than $30M_\odot$ during star formation within GCs (BJK17).

The plan of the paper is as follows. We describe the models for initial 3D distributions of gas from 1G stars and for star formation from dense gas clouds in §2. We present the results of numerical simulations of gas clump formation in GCs in §3. Based on these results, we provide several

Table 2. The parameter values for a GC in a representative models without star formation.

Stellar mass	$3.1 \times 10^5 M_\odot$
Scale length of the Plummer model	2 pc
Lower-mass cut-off (m_l) for stars	$0.1 M_\odot$
Upper-mass cut-off for stars (m_u)	$120 M_\odot$
Gas mass	$3000 M_\odot$
Gas disk size	1 pc
Mass resolution (gas)	$0.01 M_\odot$
Spatial resolution	0.014 pc
SB effect	Yes
SN and AGB feedback from 2G stars	No

implications of the present results in the context of MSPs within GCs in §4. We summarize our conclusions in §5. In this paper, we focus exclusively on star formation from gas that is either from external gas accretion or from AGB stars. We do not discuss star formation from gas within GC-hosting molecular clouds that are chemically polluted by stellar winds of massive stars, though our previous simulations demonstrated that such star formation can be important for the abundance spreads in He and CNO within GCs (e.g., Bekki & Chiba 2007).

2 THE MODEL

2.1 The AGB scenario

2.1.1 Gas accumulation

We adopt the ‘‘AGB scenario’’ in which AGB ejecta from 1G can be converted into new stars to become 2G (e.g., D’Antona et al. 2002; Bekki et al. 2007, B07: D08). In this scenario, AGB ejecta from 1G stars within GCs can be mixed with pristine gas (with the chemical abundances being the same as those of 1G stars), though such mixing is not necessary for some GCs. The total gas mass (M_g) within a GC is accordingly as follows:

$$M_g = M_{\text{acc}} + M_{\text{agb}} \quad (1)$$

where M_{acc} is the total mass of pristine gas that have the same chemical abundances as those of the GC’s host giant molecular cloud (GMC) and is accreted on the GC’s central region and M_{agb} is that of gas ejected from AGB stars. M_{acc} is further divided into (i) the total mass of gas that is left from 1G star formation within the GMC (‘‘internal’’) and (ii) that of gas that is initially outside the GC (‘‘external’’, e.g., ISM) as follows:

$$M_{\text{acc}} = M_{\text{acc,int}} + M_{\text{acc,ext}} \quad (2)$$

Although B17b has shown that most of the remaining pristine gas within GC-hosting GMCs can be expelled by energetic multiple SNII, it could be possible that a minor fraction of the remaining gas can be retained within very massive GC-hosting GMCs.

The total mass of AGB ejecta is divided into (i) the total mass of gas from AGB stars within the GC (‘‘internal’’) and (ii) that of AGB stars that do never belong to the GC (‘‘external’’) as follows:

$$M_{\text{agb}} = M_{\text{agb,int}} + M_{\text{agb,ext}} \quad (3)$$

If GCs are formed in the central regions of dwarf galaxies

[h]

Table 3. Description of the model parameters for 20 models investigated in the present study.

Model ID	$M_{\text{gc}} (M_\odot)$	$M_g (M_g)$	comments
MN1	3.1×10^5	1.0×10^3	
MN2	3.1×10^5	3.0×10^3	fiducial
MN3	3.1×10^5	5.0×10^3	
MN4	3.1×10^5	1.0×10^3	W/O SB
MN5	3.1×10^5	3.0×10^3	W/O SB
MN6	3.1×10^5	5.0×10^3	W/O SB
MN7	–	1.0×10^3	No 1G stars
MN8	–	3.0×10^3	No 1G stars
MN9	–	5.0×10^3	No 1G stars
M1	3.1×10^5	1.0×10^2	
M2	3.1×10^5	3.0×10^2	
M3	3.1×10^5	1.0×10^3	
M4	3.1×10^5	3.0×10^3	
M5	3.1×10^5	5.0×10^3	
M6	3.1×10^5	1.0×10^3	$R_{\text{gc}} = 6.9$ pc
M7	1.5×10^5	1.0×10^2	
M8	1.5×10^5	3.0×10^2	
M9	1.5×10^5	1.0×10^3	
M10	1.5×10^5	3.0×10^3	
M11	1.5×10^5	5.0×10^3	
M12	1.5×10^5	1.0×10^3	$R_{\text{gc}} = 20$ pc
M13	3.1×10^4	1.0×10^2	
M14	3.1×10^4	3.0×10^2	
M15	3.1×10^4	1.0×10^3	
M16	3.1×10^4	3.0×10^3	
M17	3.1×10^4	1.0×10^2	$R_{\text{gc}} = 4.6$ pc
M18	3.1×10^4	1.0×10^2	$R_{\text{gc}} = 6.9$ pc
M19	3.1×10^3	1.0×10^3	
M20	3.1×10^2	1.0×10^3	
M21	8.1×10^5	3.0×10^3	
M22	8.1×10^5	5.0×10^3	
M23	8.1×10^5	1.0×10^4	
M24	8.1×10^5	5.0×10^4	
M25	1.6×10^6	1.0×10^3	
M26	2.3×10^6	3.0×10^3	
M27	2.3×10^6	5.0×10^3	
M28	2.3×10^6	1.0×10^4	
M29	2.3×10^6	5.0×10^4	
M30	3.1×10^5	1.0×10^3	
M31	3.1×10^5	3.0×10^2	W/O SB
M32	3.1×10^5	1.0×10^3	W/O SB
M33	3.1×10^5	3.0×10^3	W/O SB
M34	3.1×10^4	1.0×10^3	W/O SB
M35	3.1×10^5	3.0×10^3	$R_g = 2$ pc
M36	3.1×10^5	3.0×10^3	$R_g = 3$ pc
M37	3.1×10^5	1.0×10^4	$R_g = 3$ pc
M38	3.1×10^5	4.0×10^4	$R_g = 3$ pc
M39	8.1×10^5	3.0×10^3	$R_g = 3$ pc
M40	8.1×10^5	3.0×10^4	$R_g = 3$ pc
M41	8.1×10^5	8.0×10^4	$R_g = 3$ pc
M42	2.3×10^6	3.0×10^3	$R_g = 3$ pc
M43	2.3×10^6	3.0×10^4	$R_g = 3$ pc
M44	2.3×10^6	1.0×10^5	$R_g = 3$ pc

embedded in massive dark matter halos, then gas ejected from field AGB stars within the dwarfs can be accumulated within GCs owing to deep gravitational potentials of the dwarfs (e.g., Bekki 2006; Maxwell et al. 2014). Our recent numerical simulations have also shown that about 30% of M_{agb} in GCs can originate from field AGB stars that never become the GC member stars (Bekki 2018). Furthermore, if a GC is formed from a group of numerous star clusters (i.e.,

hierarchical star cluster complex), then AGB ejecta from some small clusters that do not finally belong to the GC can be also accreted onto the GC (B17a). Thus, field AGB stars in GC-hosting galaxies can contribute significantly to $M_{\text{agb,ext}}$. In the present study, we do not specify the relative contribution of these $M_{\text{agb,int}}$ and $M_{\text{agb,ext}}$.

The most important parameter in the present study is the mass fraction of gas within GCs, which is as follows:

$$f_g = M_g/M_{\text{GC}}, \quad (4)$$

where M_{GC} is the total stellar mass of a GC. If $M_g = M_{\text{agb,int}}$, then f_g is time-dependent and a function a number of parameters, such as the stellar initial mass function (IMF) and the gas accretion timescales within GCs (Fig. 1 in B11). This f_g can be as large as 0.05 for the Salpeter IMF $\sim 10^8$ yr after the formation of 1G stars (B11). As discussed by D08 and D16, prompt SNIa can start to expel all of the gas within GCs $\sim 10^8$ yr after 1G formation. Therefore, the maximum possible f_g could be ~ 0.05 , if $M_g = M_{\text{agb,int}}$.

2.1.2 Time sequence of star formation

Fig. 1 illustrates the time sequence of discrete multiple star formation within GCs in the AGB scenario. This is only for the case of GCs which form three generations of stars (1G, 2G, and 3G); it should be noted here that some GCs have only two or four generations depending on the gas accretion histories of the GCs. As discussed in detail later in this paper, a threshold f_g ($f_{g,\text{th}}$) or M_g ($M_{g,\text{th}}$) above which star formation is possible is the key parameter that determines the star formation history of a GC. Also, as discussed in BJP17, the upper-mass cut-off of the IMF (m_u) during each episode of star formation can control the duration of the episode. The time sequence of star formation in the AGB scenario is described as follows (The starting time, $T = 0$, corresponds to the onset of star formation within GMC below). First, the formation of 1G stars starts within a fractal giant molecular cloud (GMC) and continues until the explosion of the most massive stars ($m_s \sim 100M_\odot$). All of the remaining gas left from 1G formation is expelled from the forming GC due to the energetic SN feedback effect: this epoch is defined as $t_{\text{sn-u},1}$.

Gas ejected from the most massive AGB stars can start to be accreted onto the central region of the GC after the least massive SN ($m_s = 8M_\odot$) explodes ($T = t_{\text{sn-1},1}$). The gas mass steadily increase and exceeds $M_{g,\text{th}}$ at some point so that the formation of 2G stars can start ($T = t_{g-\text{th},2}$). Therefore, there should be a time lag between the commencement of gas accretion from AGB stars and that of active star formation from the accreted gas within GCs. This time lag could be longer than the timescale of star formation from the accreted gas within GCs.

This period of no star formation is denoted as ‘‘fallow period’’ ($\Delta t_{f,1}$) in the AGB scenario, and the first fallow period is as follows:

$$\Delta t_{f,1} = t_{g-\text{th},2} - t_{\text{sn-u},1}. \quad (5)$$

The lifetime of the most massive star in each star formation episode can be different due to different m_u . Also, the timescale of M_g to exceed $M_{g,\text{th}}$ can be different in different star formation episodes. Therefore, $\Delta t_{f,i}$, where i represents

i -th generation of stars, can be different between different star formation episodes.

The formation of 2G stars is truncated by energetic feedback effects of the most massive SNII of 2G, and the duration of 2G formation ($\Delta t_{\text{sf},2}$) is given as follows.

$$\Delta t_{\text{sf},2} = t_{\text{sn-u},2} - t_{g-\text{th},2}. \quad (6)$$

Star formation from accreted gas can continue as long as M_g exceeds $M_{g,\text{th}}$. This $\Delta t_{\text{sf},2}$ depends strongly on m_u , which determines the lifetime of the most massive star. For the i -th generation of stars, $t_{\text{sf},i}$ is as follows:

$$\Delta t_{\text{sf},i} = t_{\text{sn-u},i} - t_{g-\text{th},i}. \quad (7)$$

In Fig. 1, the formation of 4G stars is not possible, because M_g cannot become larger than $M_{g,\text{th}}$, before the gas is expelled by SNIa. The cessation of star formation by SNIa has been already suggested in the earlier models based on the AGB scenario (D08, D16). Star formation from AGB ejecta can be also truncated by delayed SNII (D16, DDV16), because recent theoretical works have shown that about 15% of core-collapse supernovae occur 50 – 200 Myr after star formation (e.g., Zapartas et al. 2017).

2.1.3 Probability of gas retention

In the AGB scenario, gas ejected from AGB stars and NSM needs to be retained for a sufficient time so that the gas (mixed with pristine gas) can be converted into new stars. Such star formation can explain the observed abundance spreads in r - and s -process elements of GCs. The probability of gas retention within GCs (P_r) depends on a number of physical parameters, such as gravitational potential wells of GCs, mass densities of ICM (ρ_{icm}), and ejection velocities of gas from stars. As shown in BT17, P_r for r -process elements from NSM can be high if ρ_{icm} is as large as 10^5 atom cm^{-3} : it depends on ρ_{icm} whether gas from NSM can be retained within GCs (BT17). The delay time distribution of NSM demonstrates that NSM can start to occur around $\sim 10^7$ yr after star formation (e.g., Fig.14 in Dominik et al. 2012). This means that gas from NSM of 1G needs to be mixed with high-density gas either from AGB stars of 1G or from ISM (i.e., no original gas can be left at the time of NSM).

Gas ejected from AGB stars with low wind velocities of ~ 10 km s^{-1} can be retained within GCs with deeper gravitational potentials. A larger amount of NSM ejecta can be retained in GCs with higher ρ_{icm} (BT17). Therefore, P_r for AGB and NSM ejecta is a function of ρ_{icm} and ϕ_{gc} as follows.

$$P_r = f(\rho_{\text{icm}}, \phi_{\text{gc}}), \quad (8)$$

where the functional form f can be investigated by numerical simulations of interaction between gas ejected from NSM and AGB stars and ICM within GCs. In order to explain the observed abundance patterns of anomalous GCs with [Fe/H] spreads, D16 considered that pristine gas mixed with ejecta from SNIa or delayed SNII can be converted into 2G stars with [Fe/H] slightly higher than that of 1G. Such self-enrichment due to SNe within GCs appears to be highly unlikely, given the large amount of energy from SNe (10^{51} erg per SN) and the relatively shallow gravitational potential wells of GCs. However, if ρ_{icm} is rather high, such SN

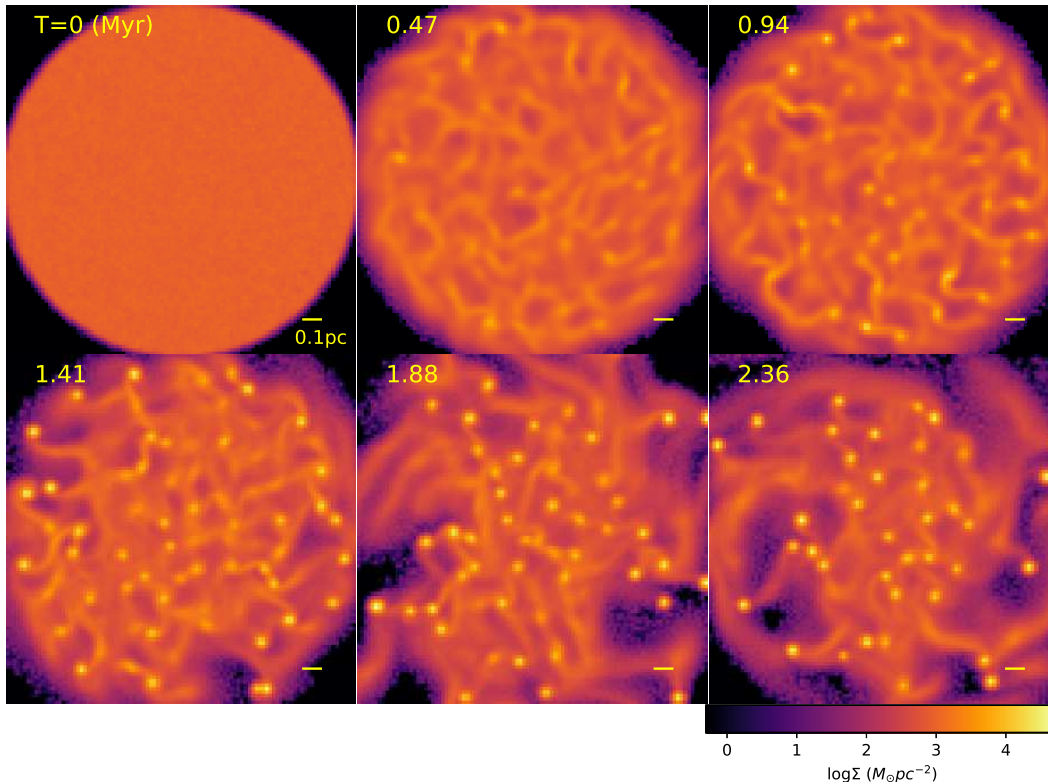


Figure 2. Time evolution of the surface mass density (Σ in logarithmic scale) of gas projected onto the x - y plane for the fiducial model MN2 without star formation. The total gas mass within the GC is $3 \times 10^3 M_\odot$, which means that the gas mass fraction (f_g) is 0.01. Time (T) that has elapsed since the start of this simulation is shown in the upper left corner of each frame. The scale bar of 0.1 pc is shown in the lower right at each panel.

ejecta could interact with ICM and consequently lose kinetic energy and momentum to finally be reaccreted onto GCs.

2.1.4 m_u as a key parameter

If the IMF in 2G (or 3G, 4G etc) is a canonical one with the slope of -2.35 and $m_u \sim 100 M_\odot$, then the duration of star formation can be very short (< 3 Myr) due to the truncation of star formation by energetic feedback effects of the massive SNe. Therefore, it is possible that only a small fraction of M_g can be converted into new stars within such a short timescale. This possibly low SFE (ϵ_{sf}) exacerbates the mass budget problem of the AGB scenario: even for ϵ_{sf} is assumed to be 1, the original GC mass (the mass of 1G stars) is by a factor of ~ 10 larger than the present-day GC mass to explain the large fraction of 2G stars for a canonical IMF. Furthermore, m_u can determine $\Delta t_{sf,i}$ ($i=1, 2$ etc), because the time lag between star formation and SN explosion of the most massive stars depends on m_u . It is possible that if m_u is less than $8 M_\odot$, star formation can continue within GCs for a quite long time until energetic events other than SNI (e.g., SNIa or delayed SNI). Thus, m_u is a key parameter

for star formation of later generations of stars (2G, 3G etc) in the AGB scenario.

It could be possible that the slope of the IMF in later generations (LG) of stars (2G, 3G etc) could be different from that of 1G owing to the formation of LG stars in dense stellar systems. If the IMF in LG (2G, 3G etc) is different from that of 1G, then the mass function (MF) of stars can be still different between 1G and LG populations even after 10 Gyr dynamical evolution. Vesperini et al. (2018) have recently investigated the evolution of the MF separately both for 1G and 2G stars within GCs using numerical simulations. They found that the initial difference of MFs between 1G and 2G can be still visible in the present-day GCs, though they evolve with time during dynamical evolution of the GCs. Such possible differences are yet to be detected observationally.

2.2 Simulation code

Based on the AGB scenario, We investigate star formation from dense gas clouds in the central regions of dense stellar systems (DSSs) such as GCs and stellar galactic nuclei using our original chemodynamical simulations codes that can be run on GPU clusters (Bekki 2013, B13; Bekki 2015,

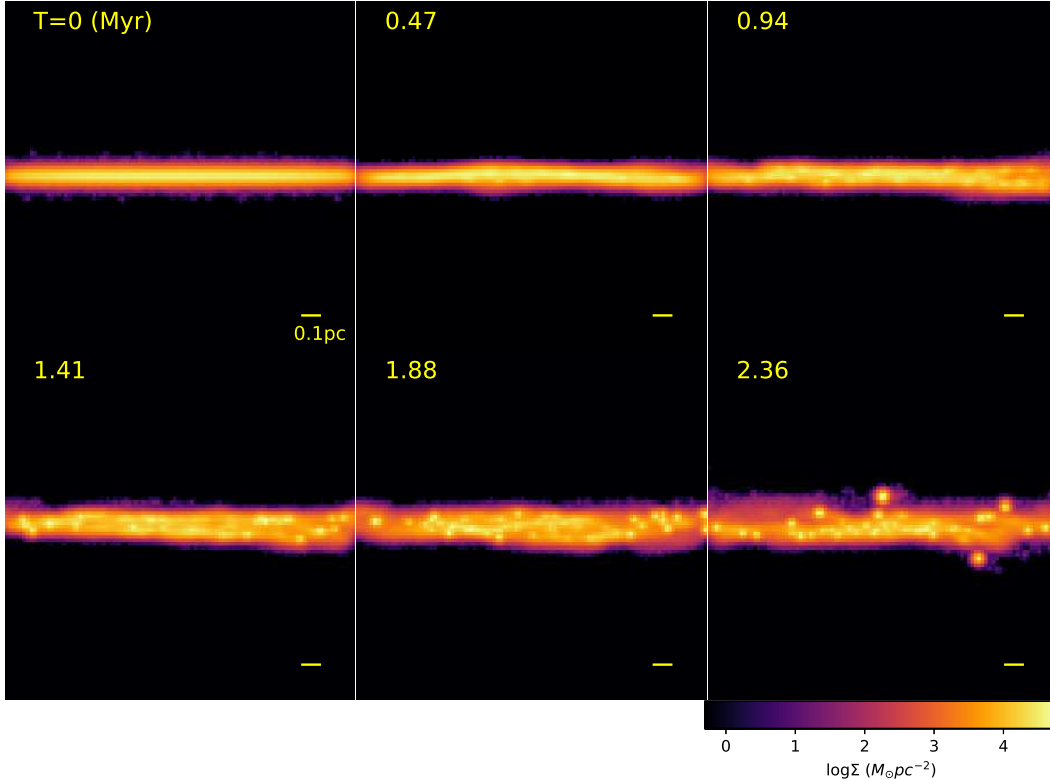


Figure 3. The same as Fig.2 but for the x - z projection.

B15). Since our main focus is not the evolution of metals and dust in galaxies and star clusters, we “switch off” the components of the code that are relevant to evolution of metals and dust. The code combines the method of smoothed particle hydrodynamics (SPH) with calculations of three-dimensional self-gravitating fluids in astrophysics. Since the details of the code are given in B13, we just briefly describe it in this paper.

It would be the best to investigate both (i) the formation of stars from fractal molecular clouds (i.e., 1G) and (ii) the formation of new stars (2G) from gas ejected from stars or from interstellar medium (ISM) in a self-consistent manner. However, our recent simulations (B17a, b) which have done this type of self-consistent simulations, do not have enough mass and size resolutions to investigate direct gravitational interaction between individual stars and small gas clouds. Therefore, we have adopted the present models in which GCs are initially in dynamical equilibrium in order to grasp some essential ingredients of such effects of star-gas interaction on secondary star formation within GCs.

2.3 Original stellar systems

We assume that an original dense stellar system has a Plummer density profile (e.g., Binney & Tremaine 1987) with a mass (M_{gc}), and a size (R_{gc}), and a central velocity disper-

sions (σ_{gc}). The scale length (a_{gc}) of the system is determined by the formula

$$a_{gc} = GM_{gc}/6\sigma_{gc}^2, \quad (9)$$

where G is the gravitational constant. Observations showed that GCs have no strong relation between M_{gc} and R_{gc} with a large dispersion of R_{gc} for a given M_{gc} (e.g., Djorgovski et al. 1997; Ashman & Zepf 2001). This no strong size-mass relation is suggested to be understood in the context of different star formation efficiencies in GCs with different M_{gc} . Therefore, we mainly investigate the models with a fixed R_{gc} that is consistent with the observed typical GC size for different M_{gc} . However, we also investigate models with different R_{gc} for a fixed M_{gc} in the present study.

The stellar system is composed of stars with different masses (not equal-mass, as assumed in B11) that follow the canonical Salpeter initial mass function (IMF) of stars. The adopted IMF in number is thus defined as follows:

$$\psi(m_l) = M_{gc,0} m_l^{-\alpha}, \quad (10)$$

where m_l is the initial mass of each individual star and the slope $\alpha = 2.35$. The normalization factor $M_{gc,0}$ is a function of M_{gc} , m_l (lower mass cut-off), and m_u (upper mass cut-off):

$$M_{gc,0} = \frac{M_{gc} \times (2 - \alpha)}{m_u^{2-\alpha} - m_l^{2-\alpha}}. \quad (11)$$

We mainly investigate the models in which m_l and m_u are

set to be $0.1M_{\odot}$ and $120M_{\odot}$, respectively. In the models with these IMF mass cut-offs, M_{gc} is $3.1 \times 10^5 M_{\odot}$ for the total number of stars (N_s) being 10^6 . We also investigate the models with higher m_1 in order to investigate GCs with higher M_{gc} for a given N_s . We particularly investigate the models with $m_1 = 0.3M_{\odot}$ and $N_s = 10^6$ (corresponding to $M_{\text{gc}} = 8.1 \times 10^5 M_{\odot}$) We particularly investigate the models with $m_1 = 0.8M_{\odot}$ and $N_s = 1.3 \times 10^6$ (corresponding to $M_{\text{gc}} = 2.3 \times 10^5 M_{\odot}$).

2.4 Gaseous distributions

Bekki (2010, B10) demonstrated that gas ejected from AGB stars of 1G populations can finally form a gas disks in the central region of the original stellar system, if 1G stars initially have a small amount of rotation: this is confirmed by B11. Our previous and recent simulations showed that gas accreted from a giant molecular cloud (GMC) onto a GC can form a compact gas disk within the GC using their new models of GMC-GC interaction (BM09; McKenzie and Bekki 2018) It is thus reasonable for the present study to assume a gas disk embedded in a DSS. In the present paper, we investigate exclusively the models in which the initial gas disks have uniform distributions with different masses (M_g) and sized (R_g).

A gas disk is represented by equal-mass gas particles with and each particle is assumed to isothermal with its temperature T_g of 10 K for most models: we do not include the time evolution of T_g of these initially cold gas particles, because any feedback effects associated with star formation (e.g., massive stars and supernovae) are not considered in the present study. This could be over simplified in gas dynamics within GCs, because AGB ejecta with temperature of more than 1000 K could heat up the existing gas. D08 showed that AGB ejecta can be cooled down to be accumulated into the central regions of GCs, though their simulations are based on 1D models (i.e., spherically symmetric distributions of gas and stars). It is beyond the scope of this paper to investigate how new AGB ejecta can influence the existing gas disk during GC evolution. For most models, the mass of each gaseous particle is set to be $0.01M_{\odot}$. Accordingly, a gas disk with $M_g = 10^4 M_{\odot}$ consists of 10^6 SPH gas particles in the present study.

The gas disk in a GC is assumed to be rotating within GCs, which is consistent with our previous simulations (B10, B11). Accordingly, i th gas particle has a circular velocity ($v_{c,i}$) determined by the gravitational potential of the GC and the gas disk as follows:

$$v_{c,i} = g(\phi(x_i)), \quad (12)$$

where x_i is the 3D position of the particle with respect to the GC's center, g is a function that determines $v_{c,i}$ from the gravitational potential ϕ . Recent observations have revealed that the Galactic GCs have a high degree of rotation with V/σ ranging from 0.1 to 0.5 (e.g., Bianchini et al. 2018). This means that the initial degree of rotation in GCs should be significantly higher than the above, because two-body relaxation effects reduce the degree (Bianchini et al. 2018). Milone et al. (2018a) have demonstrated that stellar kinematics of 2G stars in 47 Tuc shows a higher degree of anisotropies and smaller tangential velocity dispersion than

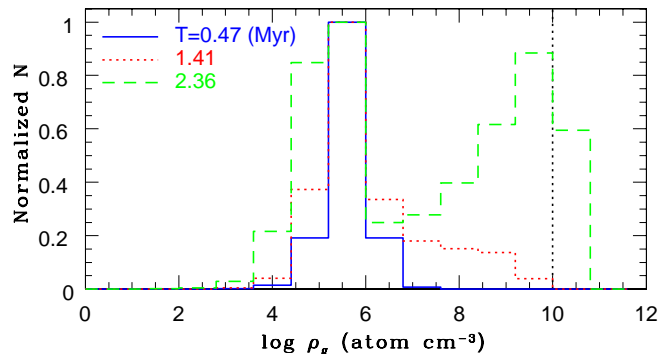


Figure 4. Distribution of gas densities (ρ_g) for the fiducial model MN2 without star formation at three different time steps, $T = 0.81$ Myr, 1.24 Myr, and 2.35 Myr. Normalized number of gas particles is given for each density bin.

1G stars and suggested that these are consistent with a formation scenario in which 2G stars originate from a compact configuration with strong rotation (e.g., Mastrobuono-Battisti & Perets 2013). These recent observations justify the adopted compact gas disks with rotation in the present study.

2.5 Star formation

Our previous simulations have already investigated star formation from gas in fractal GMCs that can form GCs with both 1G and 2G stars (B17b). The spatial resolution of the simulation is high enough to identify high-density gas with the mass density of $\sim 10^5$ atom cm^{-3} , which corresponds to cores of GMCs. In the present study, we consider that if the gas density of a particle can become higher than the typical density of first stellar cores (10^{10} atom cm^{-3}), then a new star can be formed. Therefore, the present simulations can resolve the formation of each individual star, which is a main different between the present study and B17b.

When the mass density of a gas particle exceeds a threshold value for star formation ($\rho_{g,\text{th}}$) in a model with star formation, then the particle is converted into a collisionless star particle. Accordingly, the present star formation model is as follows:

$$\rho_g > \rho_{g,\text{th}}, \quad (13)$$

where $\rho_{g,\text{th}}$ is set to be 10^{10} atom cm^{-3} , which corresponds to the mass density of first stellar cores (e.g., Meyer 1978). The mass of the new stellar particle (m_{ns}) is always the same as m_g of its original gas particle, because no gas ejection from the new star is included in the present study. We investigate the star formation of a model over 2.4 Myr in the present study. We however confirm that star formation becomes very small after ~ 3 Myr owing to rapid consumption of gas by star formation in a model with ~ 30 Myr evolution. This means that the long-term evolution of gas and star formation is not so important in discussing the star formation process within GCs in the present models.

2.6 Representative models

We investigate star formation processes within GCs for models with different M_{gc} , $R_{\text{gc}} (= 5a_{\text{gc}})$, M_g , and R_g . In order

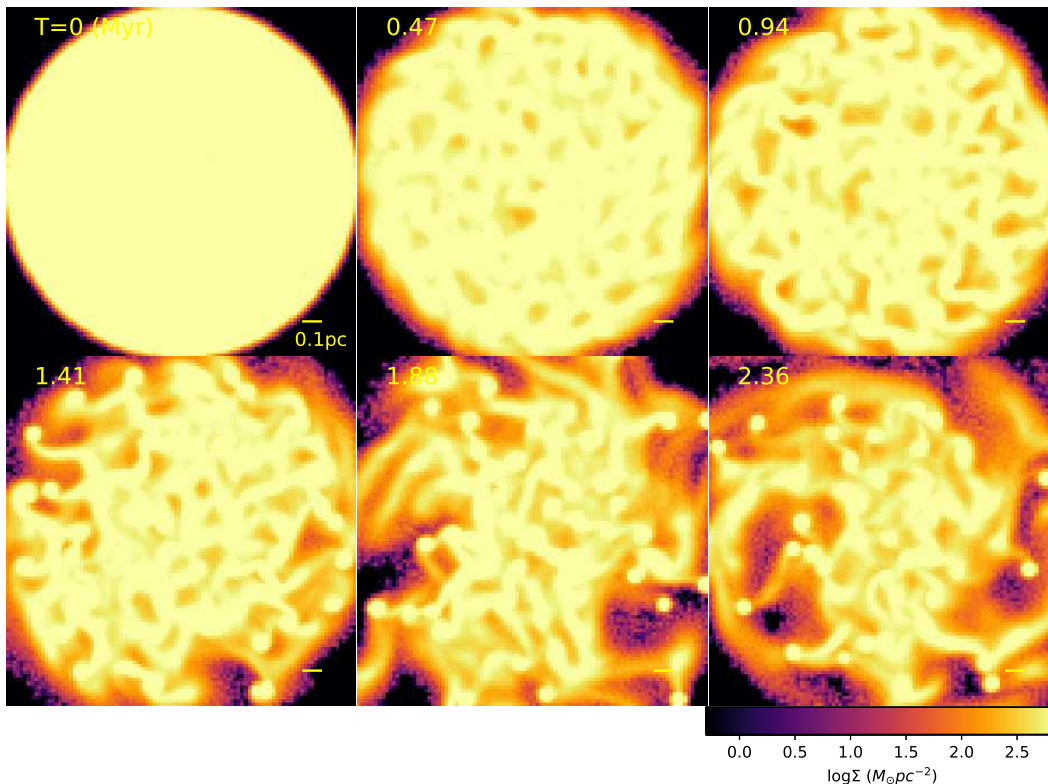


Figure 5. The same as Fig. 1 but for the model MN1 with lower gas mass fraction ($f_g = 0.003$)

to demonstrate the effects of SB on secondary star formation more clearly, we also investigate the models with and without SB. In the models without SB, the gravitational potentials of the GCs are fixed (i.e., no stellar motion) during the simulations. We also investigate the models in which star formation is not included, in order to demonstrate the effects of SB on the formation of high-density gas clumps more clearly. These models without SF are labeled as “MN” (e.g., MN1) whereas those with SF are labeled as “M” (e.g., M1)

The model MN2 with $M_{gc} = 3.1 \times 10^5 M_\odot$, $R_{gc} = 2$ pc, $M_g = 3000 M_\odot$ (and without star formation) is denoted as the fiducial model. This model and other MN models are investigated in detail, because the effects of SB on the mass growth of small (star-forming) gas clumps are crucial in the present study. The basic model parameters for the fiducial model are given in Table 2. We mainly investigate the models with star formation and $M_{gc} = 3.1 \times 10^5 M_\odot$, which is similar to the present-day typical GC mass. It should be noted that M_{gc} is the total mass of stars and compact objects (stellar mass black holes and neutron stars) in a GC after explosions of all SNII.

We also investigate star formation processes in high-mass GC models in which M_{gc} is as large as or larger than $10^6 M_\odot$, because previous theoretical models predicted that original GC masses should be at least [5 – 10] times larger than the present-day typical GC mass (e.g., Bekki & Norris

2006; D08). In these models, the lower-mass cut-off of the IMF (m_1) is set to be larger than $0.1 M_\odot$ so that M_{gc} can be larger for a given IMF slope and a total number of stellar particles. The values of physical parameters for all models are summarized in Table 3.

2.7 Resolution issues

Previous studies investigated resolution requirements for accurate simulations of the formation of collapsed objects in circumstellar disks (e.g., Bate & Burkert 1997; Truelove et al. 1997; Nelson 2007). Although these study are not directly related to the present study, their results are useful in discussing whether the new results in the present study are due to numerical artifacts. The Jeans mass (M_J) in the model M4 with $M_g = 3000 M_\odot$ is $3.7 M_\odot$ at $T = 0$, and it is much larger than the mass resolution of the simulation ($0.01 M_\odot$). M_J is even higher for models with lower M_g : it is $11.7 M_\odot$ for $M_g = 300 M_\odot$. Therefore, the present simulations can properly investigate the formation of gas clumps in a gas disk embedded in a dense stellar system.

Truelove et al. (1997) defined the “Jeans number” (J) as follows:

$$J = \frac{\Delta x}{\lambda_J} \quad (14)$$

where Δx and λ_J are the cell size of a simulation and Jeans

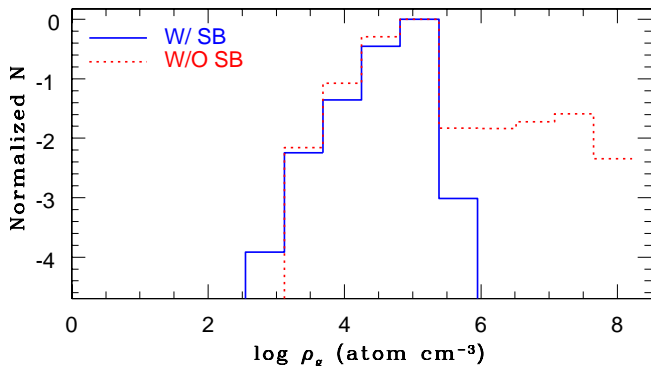


Figure 6. The same as Fig. 4 but for the model MN1 with SB and MN4 without SB at $T = 0.94$ Myr.

length, respectively. They thereby demonstrated that if J is kept lower than 0.25, then artificial fragmentation of a gas cloud can be avoided. The present simulation code is quite different from those adopted in Truelove et al. (1997). We therefore redefine J as follows:

$$J = \frac{\epsilon_g}{\lambda_J} \quad (15)$$

where ϵ_g is the gravitational softening length of gas particles (corresponding to spatial resolution). The Jeans number J is estimated to be 0.044 for models with $M_g = 3000M_\odot$ at $T = 0$ and it is lower in the models with lower M_g in the present study. Therefore, the formation of high-density clumps is not due to artificial fragmentation caused by the discreteness in the initial gas distributions of simulations.

3 RESULTS

3.1 Effects of stellar bombardment (SB)

Fig. 2 shows how high-density gas clumps can be developed during the evolution of a gas disk embedded in a GC for a fiducial model MN2 with $M_{gc} = 3.1 \times 10^5 M_\odot$ and $a_{gc} = 2\text{pc}$ ($R_{gc} = 10\text{pc}$), and $M_g = 3 \times 10^3 M_\odot$, and $R_g = 1\text{pc}$. Clearly, numerous small gas clumps with the surface densities as high as $10^5 M_\odot \text{pc}^{-2}$ can be developed from local gravitational instability around $T = 1.4$ Myr. The sizes of these high-density clumps appear to be similar in this figure, and they do not merge frequently with one another to form more massive clumps. Dynamical friction of these clumps against GC member stars cannot be efficient within a timescale of 10^6 yr, which ends up with no strong concentration of gas in the GC's center. As shown in Fig. 3, a few gas clumps cannot stay in the original thin gas disk, because they interact with other gas clumps and with individual stars intruding into the gas disk from various directions.

Using the stability criteria for a uniformly rotating isothermal disk (Goldreich & Lynden-Bell 1965), the origin of the dense gas clump formation described above can be discussed as follows. The stability parameter for gas (Q_g) is described as follow:

$$Q_g = \frac{v_s \Omega}{G \Sigma_g} \quad (16)$$

where v_s , Ω , G , and Σ_g are the sound velocity, angular speed, gravitational constant, and surface density of gas,

respectively. If this Q_g is less than 1.06 in a gas disk, then the disk becomes unstable. It is found that (i) Q_g ranges from 1.04 ($r = 1\text{pc}$) to 1.64 (0.1 pc) in this model and (ii) it is lower than 1.06 in the outer part of the disk. This means that the gas disk is marginally stable against local disk instability. However, the formation of dense gas clumps (and the subsequent star formation) is possible due to local instability in the regions with lower Q_g : clump formation can proceed more efficiently in the outer region with lower Q_g . The models with lower M_g ($\leq 1000M_\odot$) have higher Q_g (> 2) so that dense gas clumps cannot be efficiently formed from local instability within the gas disks.

Fig. 4 describes how high-density gas clumps can be gradually developed in the gas within a timescale of Myr. Only a small fraction of gas particles can have gas densities (ρ_g) larger than $10^{10} \text{atom cm}^{-3}$ corresponding to first stellar cores (i.e., a threshold gas density for star formation) at $T = 1.41$ Myr. A significant fraction of gas particles can finally have $\rho \sim 10^{10} \text{atom cm}^{-3}$ at $T = 2.36$ Myr, which implies that star formation cannot start soon after gas accretion from AGB stars or ISM onto GCs. It should be noted here that most of previous models for multiple stellar populations of GCs (e.g., B07, D08, BJP17) assumed star formation soon after gas accretion in GCs (i.e., no time delay between gas accretion and star formation is assumed).

It should be noted here that no initial turbulence is introduced in the original gas disks in these models. Therefore, the formation of high-density gas clumps and the subsequent star formation in these models should be quite different from those in fractal gas clouds with initial turbulence investigated in previous studies (e.g., Klessen et al. 1998; Dale 2011). Therefore, the present study, for the first time, has demonstrated that star formation is possible from gas without turbulence. As described in later for the models with star formation, a certain fraction of gas particles can have $\rho_g \geq 10^{10} \text{atom cm}^{-3}$ at 0.47 Myr, which means that hydrodynamical pressure of gas can suppress the mass growth of gas clumps in the MN models without SF.

Fig. 5 shows the formation of gas clumps in the model MN1 in which all model parameters except M_g are the same as those adopted in MN2. Clearly, the surface densities (Σ_g) of gas clumps in this model with lower M_g are much (by almost two orders of magnitude) lower than those in MN2, which implies that f_g is a key factor which determines whether star formation is possible. Star formation can be significantly delayed or not be possible in GCs with lower f_g (< 0.01). This possible threshold f_g for star formation can have several important implications on the origins of multiple stellar populations, as discussed later in this paper.

In order to demonstrate the negative effects of SB on secondary star formation more clearly, we have investigated models without SB. Fig. 6 describes how SB can influence the formation of high-density clumps in the early evolution of gas in a GC for the models MN1 with SB and MN4 without SB. The model with SB does not show any gas particles with $\rho_g > 10^6 \text{atoms cm}^{-3}$, which means that the mass growth of gas clumps can be severely suppressed in this model with lower M_g ($= 1000M_\odot$). However, there are no significant differences in the normalized distributions of ρ_g between the two models for $\rho_g < 10^5 \text{atom cm}^{-3}$. These results clearly demonstrate that star formation processes such

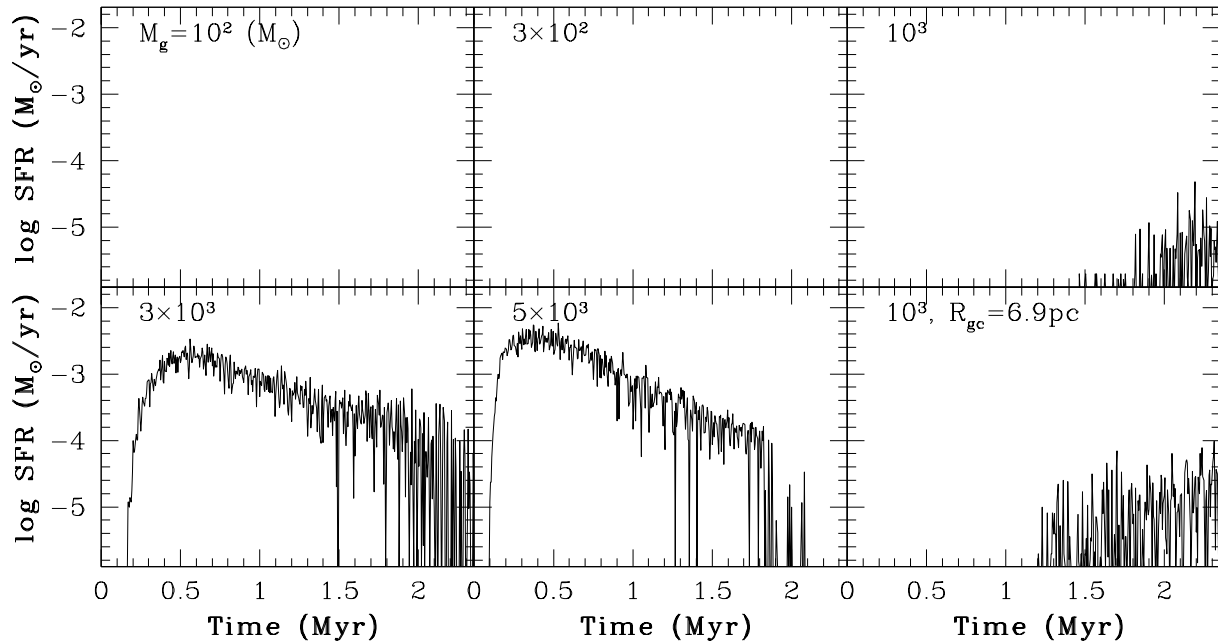


Figure 7. Time evolution of star formation rates for six different models with $M_{\text{gc}} = 3.1 \times 10^5 M_{\odot}$. The initial GC size (R_{gc}) is the same between the models ($R_{\text{gc}} = 10\text{pc}$) except the model shown in the lower right (6.9pc). The initial gas mass is shown in the upper left corner of each panel.

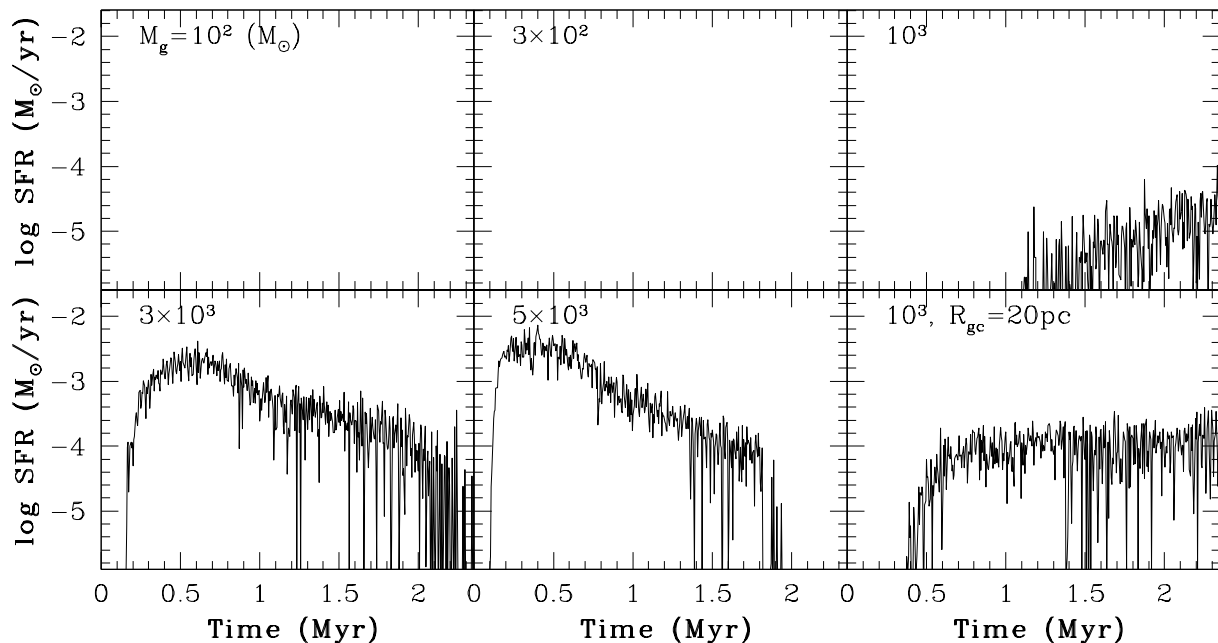


Figure 8. The same as Fig. 6 but for $M_{\text{gc}} = 1.5 \times 10^5 M_{\odot}$.

as the mass fraction of gas converted into new stars and the timescale of star formation can be influenced by SB when f_{g} is low. It is confirmed that this SB effect is not seen in the models with $f_{\text{g}} \geq 0.01$.

3.2 Star formation in different models

Fig. 7 describes how the star formation histories within GCs depends on M_{gc} and R_{gc} in the models M1-M6. Sec-

ondary star formation is either completely shut down or very severely suppressed due to SB and gravitational potentials of existing stars in the models with $f_{\text{g}} < 0.01$ (i.e., M1, M2, and M3), and this effect can be also seen in the model M6 with a very compact GC. These results confirm that f_{g} is the most important parameter for secondary star formation. The model M4 with $f_{\text{g}} = 0.01$ shows a bursty star formation with $\sim 80\%$ of the initial gas being converted into new stars (i.e., $\epsilon_{\text{sf}} = 0.8$) within ~ 2 Myr. This timescale of star formation is shorter than the lifetime (~ 3 Myr) of the most

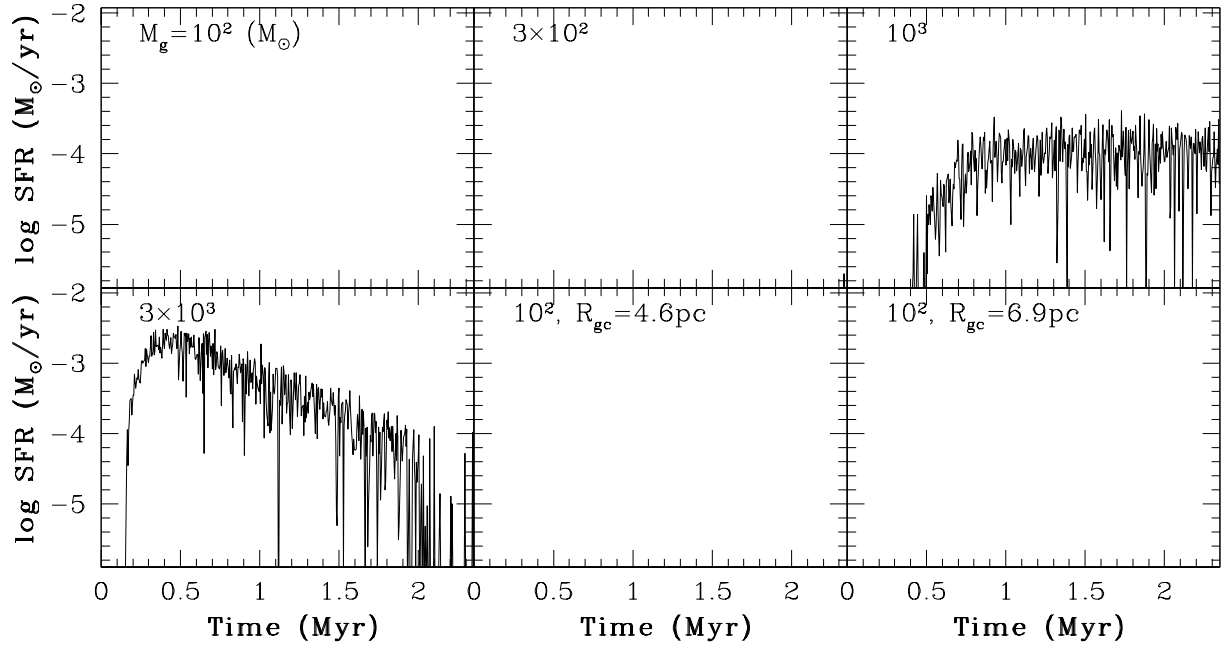


Figure 9. The same as Fig. 6 but for $M_{\text{gc}} = 3.1 \times 10^4 M_{\odot}$. Two models with different R_{gc} are shown.

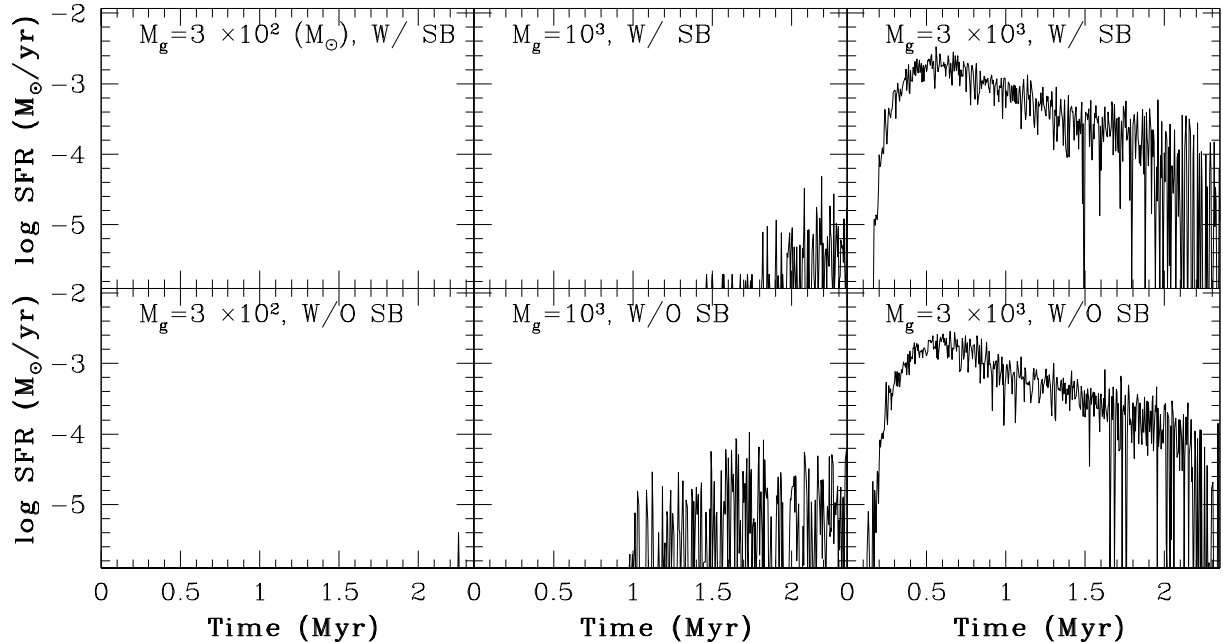


Figure 10. The same as Fig. 6 but for the models with SB (upper three) and without SB (lower three). In these models, $M_{\text{gc}} = 3.1 \times 10^5 M_{\odot}$ and $R_{\text{gc}} = 10 \text{pc}$.

massive stars adopted in the present study ($120 M_{\odot}$). Such short and bursty star formation from gas within GCs ensures that secondary star formation cannot be interrupted by SNI before the consumption of most of the gas. These results demonstrate that there is a threshold gas fraction ($f_{\text{g,th}}$) above which short and bursty star formation is possible.

Fig. 8 confirms that GCs with lower f_{g} do not show short bursty star formation in the models with $M_{\text{gc}} = 1.5 \times 10^5 M_{\odot}$. However, the model M9 with lower GC masses

shows weak star formation for $f_{\text{g}} = 0.006$, which is a hint for a higher $f_{\text{g,th}}$. The model M12 with lower f_{g} and larger R_{gc} (thus less compact) shows significantly more star formation than M9 with the same f_{g} yet smaller R_{gc} . This more efficient star formation in less compact stellar systems implies that the degree of self-gravitation in gas (i.e., $M_{\text{g}}/M_{\text{gc}}$) within R_{gc} is crucial for star formation in GCs. For this model M12, star formation can continue with an almost constant star formation rate for a longer timescale due to the lower star formation efficiency.

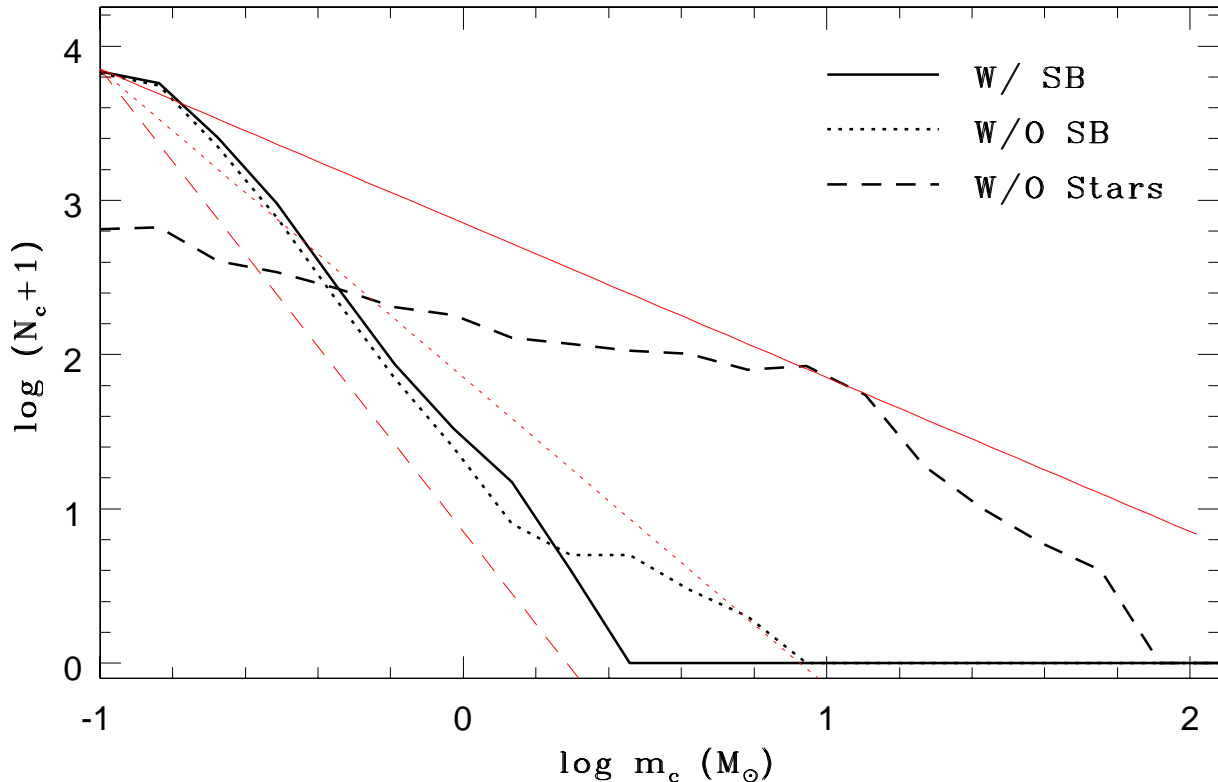


Figure 11. Number distributions (N_c) of gas cloud masses (m_c) for the models with $M_{gc} = 3.1 \times 10^5 M_\odot$ and $f_g = 0.01$ (black solid line) at $T = 0.47$ Myr. For comparison, the same models yet without SB (dotted) and without stars and compact stellar objects (dashed) are shown. The model labeled as “W/O stars” accordingly means that there is no global gravitational field of a GC. For convenience, $\log(N_c + 1)$ is shown in this figure. The three slopes of the cloud mass functions, $\alpha_c = -1$ (red solid), -2 (dotted), and -3 (dashed) are also shown for comparison.

Table 4. Star formation efficiencies (ϵ_{sf}) for the representative models with different f_g and R_g .

$M_{gc} (M_\odot)$	R_g (pc)	f_g	ϵ_{sf}
3.1×10^5	1	0.01	0.73
3.1×10^5	2	0.01	0.30
3.1×10^5	3	0.01	0.12
3.1×10^5	3	0.1	0.47
8.1×10^5	1	0.006	0.70
8.1×10^5	3	0.03	0.36
8.1×10^5	3	0.1	0.49
2.3×10^6	1	0.002	0.46
2.3×10^6	3	0.005	0.07
2.3×10^6	3	0.05	0.45

Although Fig. 9 confirms that there is $f_{g,th}$ in GCs with and $M_{gc} = 3.1 \times 10^4 M_\odot$, the model with $f_g = 0.01$ ($M_g = 3 \times 10^2 M_\odot$) does not show any star formation, which is in a striking contrast with M4 with $f_g = 0.01$ that shows short bursty star formation. Although star formation is relatively active in the model with $f_g = 0.03$, it proceed gradually with an almost constant rate without burst. This is quite different from the more massive models with $f_g = 0.03$ and $M_{gc} = 3.1 \times 10^5 M_\odot$. The model with $f_g = 0.1$ shows a similar short bursty behavior like M8, which demonstrates that $f_{g,th}$ should be larger for GCs with lower masses. It should be noted here, however, that $f_g = 0.1$ is possible only if almost all AGB ejecta is accumulated in GCs for a canonical (Salpeter) IMF (see Fig. 1 in B11). Therefore, it is reason-

able to say that low-mass GCs are unlikely to show short bursty star formation from gas accumulated from AGB stars within the GCs. If such low-mass GCs show short bursty star formation, then gas should be supplied from outside GCs (e.g., ISM).

GCs with $f_g = 0.003$ do not show star formation in the models with $M_{gc} = 3.1 \times 10^4 M_\odot$ irrespective of R_{gc} , as shown in Fig. 9. This suggests that the gas density above which star formation can start within GCs is higher for low-mass GCs. These results shown in Figs. 7-9 suggest that secondary star formation can start earlier (i.e., when f_g is lower) in more massive GCs. These also suggest that efficient star formation is not possible in low-mass GCs with $M_{gc} < 10^5 M_\odot$, even if gas can be accumulated in the central regions of the GCs. It should be noted here that these low-mass GCs are less likely to retain AGB ejecta owing to the lower escape velocities (B11).

Fig. 10 demonstrates that GCs show lower star formation rates in the model M3 with SB than in M32 without SB for $f_g = 0.003$. This suppression of star formation due to SB can be barely seen in the models M2 with SB and M31 without SB for $f_g = 0.001$. For these models with low f_g , global potentials of GCs alone can suppress star formation. Very low star formation in the model without SB for low f_g means that the threshold f_g for the onset of star formation is lower for the models without SB. The models M4 and M33 with and without SB, respectively, do not show any significant differences in their star formation histories, which

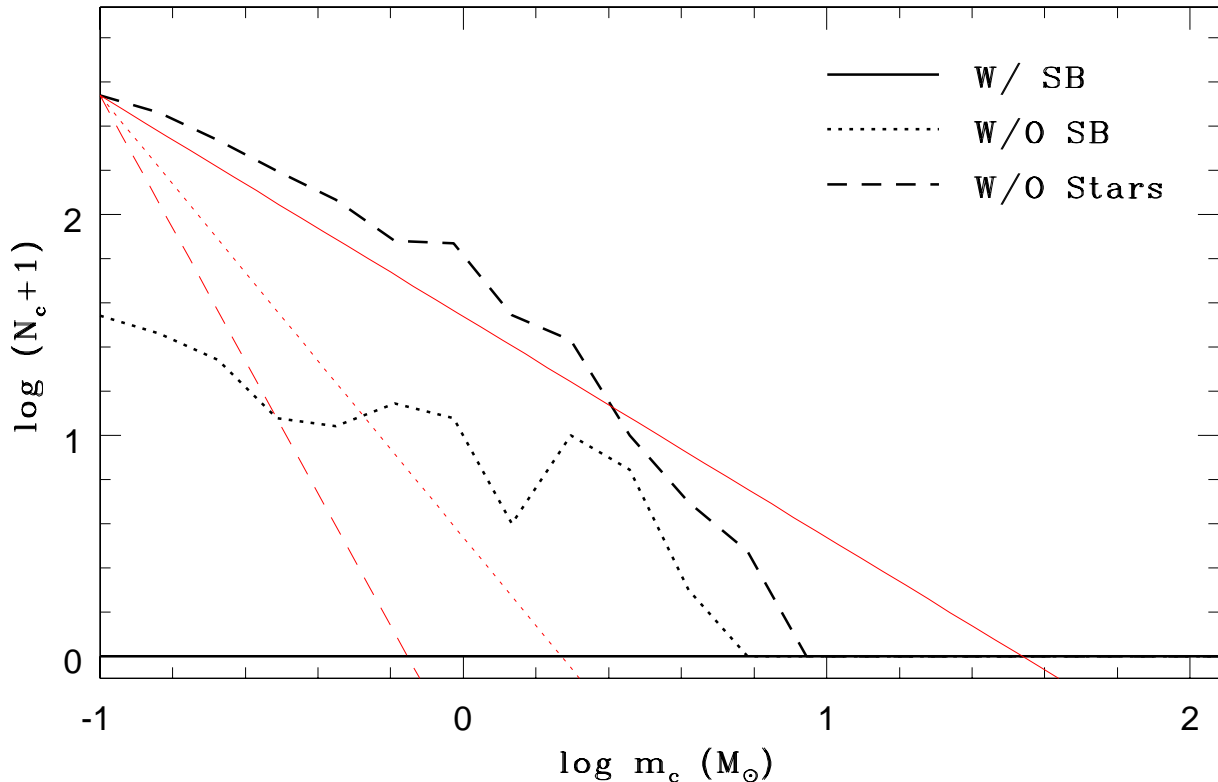


Figure 12. The same as Fig. 11 but for the models with $f_g = 0.003$ at $T = 0.94$ Myr. No gas clouds that are collapsing and have masses more than $0.1M_\odot$ are found in the model with SB (i.e., solid line).

demonstrates that SB is not important for GCs with higher f_g . In these models, the larger degree of self-gravitation in gas can cause more rapid growth of high-density gas clumps within GCs so that star-gas direct interaction cannot greatly influence the formation and evolution of gas clumps. Thus, secondary star formation within GCs can be influenced by SB only when f_g is low (< 0.01): SB can influence the star formation process only in the early phase of GCs with gas.

Table 4 summarizes ϵ_{sf} for more massive GC models with M_{gc} ranging from $3.1 \times 10^5 M_\odot$ to $2.3 \times 10^6 M_\odot$. First, it is clear that ϵ_{sf} is quite high (> 0.4) for all models with $f_g \geq 0.01$ and $R_g = 1$ pc, which suggests that star formation can proceed in a bursty manner even in the earlier phases of gas accretion within GCs. Second, massive GCs with $M_{gc} \geq 8.2 \times 10^5 M_\odot$ show $\epsilon_{sf} > 0.7$ even for $f_g = 0.006$. Since, the mass ratio of gas from massive AGB stars with $m_s \geq 7M_\odot$ to the original GC mass is about 0.008 for a canonical IMF (adopted in this study) and a mass fraction of AGB ejecta (lost to ICM) being 0.8, this result means that if ICM originates exclusively from AGB stars, then star formation is possible directly from gas ejected from massive super AGB stars with masses larger than $7M_\odot$.

Third, ϵ can be lower in the models with larger R_g (2pc and 3 pc) which correspond to GCs with a larger amount of angular momentum in their gaseous components. Although ϵ_{sf} is not so low (~ 0.3), f_g should be significantly larger for larger R_g for high ϵ_{sf} (> 0.5). For example, ϵ_{sf} is ~ 0.5 even if f_g is 0.11 in the models with $M_{gc} = 3.1 \times 10^5 M_\odot$ and $R_g = 3$ pc. This required high f_g can be achieved only if almost all gas from massive and intermediate-mass AGB stars can be accreted onto GCs. This accordingly suggests

that it is unlikely for larger gas disks to form new stars with high ϵ_{sf} (> 0.5). Since the gas disk sizes within GCs can be determined by the initial angular momentum of their 1G stars (B11), the above result implies that angular momentum of GCs can be a key determinant for star formation within GCs.

3.3 Mass functions of gas clumps

The models without star formation are the best to demonstrate the effects of SB on the mass growth of small clumps and the mass function (MF) of the clouds within GCs more clearly. We here describe the results for two representative models with $M_{gc} = 3.1 \times 10^5 M_\odot$ and $f_g = 0.003$ and 0.01. As shown in Fig. 11, the MF of gas clumps developed from local instability within GCs is not so much different between the models with and without SB for lower masses ($m_c < 3M_\odot$) at $T = 0.47$ Myr, when star formation can be very active if star formation is included. However, there are no massive clumps with $m_c > 3M_\odot$ in the model with SB, which suggests that the formation of more massive stars with $m_c \geq 3M_\odot$ can be suppressed by SB. The slope of the MF (α_c) is approximately -2.5 for $m_c < 3M_\odot$ at $T = 0.47$ Myr for the two models.

The comparative model without stars (i.e., no gravitational potential of a GC) shows a quite flat MF of clouds for $m_c < 10M_\odot$ and a significant fraction of massive clouds with $m_c \geq 8M_\odot$. The initial rotating gas disk is initially unstable ($Q_g < 1$) so that massive numerous gas clumps can be developed rapidly from local instability. This model is introduced such that the physical roles of background potential of stars

in the formation of gas clumps (thus gas mass function) can be more clearly shown. These results suggest that massive star formation that leads to SNII can be severely suppressed by a combination of star-gas interaction and gravitational potentials of GCs. These furthermore imply that the IMF can be “top-light” in secondary star formation within GCs and thus that SNII feedback effects on gas left after the formation of preceding generations of stars are less dramatic owing to the smaller number of massive stars. If the formation of gas clumps with $m_c \geq 8M_\odot$ is completely suppressed, then secondary star formation can continue until all of the gas is consumed.

Fig. 12 shows that no high-density gas clumps with $m_c \geq 0.1M_\odot$ can be formed at $T = 0.94$ Gyr in the model with $f_g = 0.003$ and SB. Its comparative model without SB, however, shows the formation of small clouds with m_c up to $\sim 6M_\odot$ and a flat mass function. Fig. 11 also confirms that the GC’s gravitational potential can strongly suppress the formation of massive small clumps with $m_c \geq 8M_\odot$. Furthermore, it is clear that the GC’s potential can suppress the formation of low-mass clumps too in the model with this low f_g , in which the degree of gaseous self-gravity is so low that gas clouds cannot grow rapidly through accretion of nearby gas. Thus, the results for the models with $f_g = 0.003$ and 0.01 demonstrate that the formation of massive stars that can explode as SNII can be severely suppressed, in particular, in the early phases of GCs with lower f_g .

4 DISCUSSION

4.1 Limitation of the models

The present study has assumed that gas accreted from AGB stars and/or ISM can have a disk structure and rotation within a GC. Although such a rotating gas disk has been demonstrated to be formed in recent simulations of GC formation (e.g., B11; BM09), it is still possible that the adopted gas disk model is over-simplified and less realistic as follows. After the formation of a disk from gas ejected from AGB stars in a GC (i.e., the formation of “existing disk”), a significant amount of ISM can be accreted onto the GC. The spin of the existing gas disk consisting of AGB ejecta would not be necessarily aligned with that of ISM accreting onto the GC, because gas accretion can be possible from any direction. The alignment of spin axes between the existing gas disk and the accreting ISM is possible, only if the spin axis of the GC is well aligned with the gas disk of the GC-hosting galaxy.

If the angular momentum vector of the accreting ISM is quite different from that of the existing gas disk, then such ISM accretion could significantly change the structure and kinematics of the existing gas disk. Accordingly, the gas disk that is assumed to be thin and rotating over ~ 3 Myr in the present study could be over-simplified. If dynamical and hydrodynamical interaction between the existing gas disk and accreting ISM can heat up the disk (i.e., high gaseous temperature), then Q_g becomes significantly larger (> 1), which ends up with suppression of star formation. Also, such interaction transforms the initially thin disk to a considerably thick one, and then star formation could be suppressed too owing to the lower surface gas density. It is our future study

to investigate how the structure and kinematics of gas originating from AGB ejecta and ISM within GCs can evolve with time for models with different spin axes of GCs with respect to spin axes of their host galaxies’ gas disks. Although such a future study requires modeling both for the evolution of galactic gas disks and for gas accretion onto GCs, it can improve our understanding of secondary star formation within GCs.

4.2 Origin of He-rich stars in massive GCs

A few massive Galactic GCs (e.g., NGC 2808 and ω Cen) are observed to have high He abundances (Piotto et al. 2005), though some other GCs show such He abundance enhancement to a lesser extent (e.g., Milone et al. 2017). A key questions related to the origin of these He-rich stars is that if they are formed from AGB ejecta with high Y , abundance enhancement to a lesser extent (e.g., Milone et al. 2017). A key questions related to the origin of these He-rich stars is that if they are formed from AGB ejecta with high Y , A key questions related to the origin of these He-rich stars is that if they are formed from AGB ejecta with high Y , A key questions related to the origin of these He-rich stars is that if they are formed from AGB ejecta with high Y , then external pristine gas with normal Y (~ 0.245) for low-metallicity GCs) should not mix with the ejecta so that Y can be kept still high for the new stars (i.e., dilution cannot occur). It has been, however, physically unclear why such star formation from gas that is not mixed with pristine gas is possible in massive GCs. Since only massive AGB stars ($m \geq 5M_\odot$) are predicted to eject gas with high Y (e.g., Ventura & D’Antona 2009; Karakas 2010), star formation should start after the AGB ejecta is accumulated yet before ejecta with lower Y from low-mass AGB stars is accumulated (to dilute the He-rich gas from massive AGB stars).

As shown in the present study, star formation can proceed very efficiently with $\epsilon_{sf} > 0.5$ in massive GCs, if the gas mass fractions (f_g) exceed 0.01. This $f_{g,th}$ of ~ 0.01 is smaller than the mass fraction of gaseous ejecta from AGB stars with $m_s \geq 5M_\odot$ for a canonical IMF. Therefore, star formation directly from gas from massive AGB stars is possible. Furthermore, such $f_{g,th}$ for star formation is found to be higher for GCs with lower masses in the present study. Since f_g can increase with time due to contributions of gas from AGB stars with different masses (thus different lifetimes), these two results imply that more massive GCs are more likely to start forming 2G stars earlier. It is therefore possible that 2G stars with high Y are formed from gas from massive AGB stars only in massive GCs. The present study did not investigate the gas accumulation processes of AGB stars with different masses and the subsequent star formation in a self-consistent manner. Thus, it is our future study to provide more quantitative predictions on the mass fractions of He-rich stars in GCs with different masses.

Although the origin of the observed discrete He-rich stellar populations (2G, 3G etc) can be understood in the context of star formation directly from AGB ejecta, recent observations have shown that even 1G stars can possibly have He abundance spreads (δY) to a lower degree (e.g., Millone et al. 2018b). The average δY of ~ 0.05 is significant, though it is smaller than δY observed in NGC 2808 and ω Cen. If the observed δY is due to the initial δY of 1G

stars (i.e., not due to stellar evolution), the AGB scenario alone cannot simply explain it. Our previous numerical simulations of GC formation within fractal GMCs showed that stellar winds from massive OB stars can chemically pollute GC-hosting GMCs, which ends up with abundance spreads in He, C, N, and O among 1G stars formed within the GMCs (Bekki & Chiba 2007). The simulated δY is typically small (~ 0.03), however, such a smaller δY is consistent with δY observed in 1G stars within GCs. We here suggest that δY observed in 1G and 2G stars of GCs is caused by star formation from gas polluted by massive stellar winds within GC-forming GMCs and by that from AGB ejecta (mixed with pristine gas), respectively.

4.3 Discrete multiple stellar populations

One of key observational results related to the origin of multiple stellar populations in GCs is that the distribution of stars along the [Mg/Fe]-[Al/Fe] anti-correlation in NGC 2808 is not continuous (Carretta 2014): NGC 2808 consists of three distinct groups with different [Mg/Fe] and [Al/Fe]. This type of discrete multiple stellar populations has been discovered in other GCs, such as NGC 6752 and M22 (e.g., Carretta et al. 2012; Milone et al. 2013; Marino et al. 2011). BJP17 proposed the following scenario that explains the origin of these discrete multiple stellar populations. First, the first generation of stars (1G) are formed from a giant molecular gas. Then, about 30 Myr after 1G formation, the second generation of new stars (2G) can be formed from AGB ejecta of 1G population. This 2G stars can last only for [10-20] Myr, because of the gas expulsion by the 2G's most massive stars with m_s significantly lower than that of the 1G's most massive stars. After the truncation of 2G star formation by SNe, the third generation (3G) of stars are then formed from AGB ejecta. Thus, the origin of discrete multiple stellar populations is due to this cycle of star formation followed by its truncation by SNe in BJP17.

It is assumed in BJP17 that (i) star formation can be resumed soon after low-mass SNe ($m = 8M_\odot$) occurred and thus (ii) the time lag between two subsequent stellar populations (t_{lag}) is $\sim 3 \times 10^7$ yr. However, as shown in the present study, these assumptions would not be so reasonable owing to $f_{g,\text{th}}$. After the total removal of remaining gas from a GC, an enough amount of gas from AGB stars needs to be accumulated so that f_g can exceed $f_{g,\text{th}}$. Therefore, t_{lag} can be significantly longer than $\sim 3 \times 10^7$ yr adopted in BJP17, which means that the discreteness in the distribution along the Mg-Al anti-correlation could be even more pronounced. Furthermore, $f_{g,\text{th}}$ suggests that star formation can be naturally truncated when f_g becomes lower than $f_{g,\text{th}}$. BJP17 adopted an assumption that all AGB ejecta is removed from the GC by some unknown physical process in order to avoid everlasting star formation. The present study suggests that there is no need for theories of GC formation to adopt an ad hoc assumption of star formation truncation thanks to $f_{g,\text{th}}$.

This scenario, however, has not demonstrated that gas chemically polluted by 1G (2G) SNe cannot participate in the formation of 2G (3G) stars: [Fe/H] should be very similar between different generations of stars to explain the observed very small [Fe/H] spreads (< 0.05 dex) for normal GCs. In particular, it is not so clear whether AGB ejecta

used for the formation of 2G stars in a GC can be completely ejected from the GC so that AGB ejecta from 2G stars for 3G formation can have almost the same [Fe/H] as 1G and 2G stars. The present study has demonstrated that if $f_g < f_{g,\text{th}}$, then star formation can be severely truncated even without SN feedback effects. Accordingly, 2G star formation is truncated when f_g becomes lower than $f_{g,\text{th}}$, and 3G star formation cannot start until f_g becomes higher than $f_{g,\text{th}}$. This provide an alternative scenario (without SN feedback effects) that the origin of discrete MSPs is closely associated with $f_{g,\text{th}}$.

If m_u is less than $8M_\odot$, then only 2G (no 3G, 4G etc) can be formed in the present AGB scenario. Accordingly, the scenario can explain the origins of GCs with discrete (e.g., NGC 2808) or continues abundance spreads self-consistently. It is not clear how other GC formation scenarios can explain the discrete MSPs observed in some GCs. Elmegreen (2017) proposed a new GC formation scenario in which stellar envelopes of high-mass 1G stars in a GC-forming GMC are stripped and then mixed with pristine gas to be finally converted into new stars with chemical abundances different from those of 1G stars. He suggested that a GC-forming GMC consists of subclumps with different self-enrichment histories, and thus that the new GC can have different discrete MSPs. GC formation scenarios like this, in which all GC stars are formed before SNII (i.e., within 3 Myr), can possibly explain discrete MSPs in GCs, however, they cannot simply explain abundances spreads in r - and s -process elements observed in some GCs: they need to invoke other physical mechanisms to explain such abundance spreads. The AGB scenario can naturally explain both the discreteness of MSPs and the abundance spreads in r - and s -process elements in a self-consistent manner.

4.4 Top-light IMFs in secondary star formation ?

The observed large fractions of 2G stars (typically ~ 0.7) in GCs have been suggested to require either original GC masses that are by a factor of ~ 10 larger than the present-day ones or a particular combination of IMFs for 1G and 2G stars (e.g., Bekki & Norris 2006; Prantzos & Charbonnell 2006). The required large mass of a GC is known as the ‘‘mass budget’’ problem, which has not been solved yet. One of possible ways to alleviate this mass budget problem is to assume that the IMF for 2G stars is top-light, because the mass fractions of low-mass 2G stars (i.e., those which can be observed in the present-day GCs) can be significantly larger than those for a canonical IMF. As shown in the present study, the formation of massive gas clumps that lead to the formation of massive stars with $m_s \geq 8M_\odot$ can be severely suppressed in GCs. The combination of a top-heavy IMF for 1G stars and a top-light IMF for 2G stars can significantly reduce the required initial masses of GCs in comparison with models with canonical IMFs both for 1G and 2G stars (Bekki & Norris 2006).

Such a top-light IMF can allow secondary star formation to last longer, because the mass (lifetime) of the most massive star in secondary star formation can be small (longer). As shown in our previous studies (B17b), star formation from AGB ejecta can continue to be efficient, only if feedback effects of SNII from 2G stars are suppressed in GCs, because such feedback effects can expel most of AGB

ejecta within GCs. Such a high star formation efficiency due to much less efficient SNII feedback effects in GC formation can increase the final mass fraction of 2G stars. Cabrera-Ziri et al. (2014) concluded that there is no star formation in massive young star clusters within disk galaxies, because no $H\beta$ and [OIII] emission from massive OB stars was found (see Goudfrooij et al. 2014 for a criticism for this interpretation of the observational results). This observed apparent lack of massive OB stars in young massive clusters does not necessarily mean the lack of star formation, if the IMF is top-light (i.e., no formation of OB stars yet formation of lower mass stars). Therefore, a top-light IMF in secondary star formation cannot only contribute to a possible solution of the mass budget problem but also can provide a hint for the apparent lack of secondary star formation in young massive star clusters.

Observations have shown that massive OB stars can be formed from direct collisions between molecular clouds (e.g., Fukui et al. 2015, 2017, 2018). Recent 3D MHD simulations of colliding molecular clouds have demonstrated that massive molecular cores, which lead to the formation of massive stars, can be efficiently developed in the shocked gaseous layers induced by cloud-cloud collisions (e.g., Inoue & Fukui 2013). Such collisions between molecular clouds formed from gas accumulated within GCs are highly unlikely. Therefore, if the major formation mechanism for OB star formation is cloud-cloud collisions, then OB stars are highly unlikely to be formed within GCs. Thus, these recent observational and theoretical studies of OB star formation through cloud-cloud collisions also suggest top-light IMFs in secondary star formation within GCs.

5 CONCLUSIONS

We have investigated whether gravitational interaction between gas and individual stars (“stellar bombardment”, SB) within a GC can influence secondary star formation in the GC using our new hydrodynamical simulations. Many models with different gas mass fractions (f_g), initial GC masses and sizes (M_{gc} and R_{gc} , respectively), and gas disk sizes (R_g) have been investigated so that the effects of SB on star formation can be discussed. The main conclusions are as follows.

(1) Small gas clouds with $\rho_g > 10^{10}$ atom cm^{-3} corresponding to first stellar cores can be formed due to local gravitational instability within gas disks without initial turbulence. Consequently, a significant fraction of the gas can be converted into new stars within a short timescale ($< 3 \times 10^6$ yr). This star formation in gas disks without initial turbulence is in a striking contrast with star formation processes due to turbulent fragmentation of self-gravitating gas clouds that have been investigated extensively in many previous works (e.g., Klessen et al. 1998).

(2) SB can suppress the growth of high-density gas clumps, if f_g is less than a threshold gas fraction ($f_{g,th} \sim 0.01$ for $M_{gc} \sim 3 \times 10^5 M_\odot$). This suppression ends up with delayed and less efficient secondary star formation in GCs with low f_g . Secondary star formation proceeds

efficiently with $\epsilon_{sf} > 0.5$ for $f_g > f_{g,th}$. This $f_{g,th}$ is smaller for larger M_{gc} , which implies that secondary star formation from gas can start earlier in more massive GCs.

(3) GCs with larger R_g show larger $f_{g,th}$ for $M_{gc} \geq 3 \times 10^5 M_\odot$. Since the original angular momentum of GCs (1G stars) can determine the sizes of gas disks (B11), this result implies that the angular momentum is one of key factors for star formation from the accumulated gas within GCs.

(4) Gas ejected from massive AGB stars can be accumulated in the central region of a GC earlier, because more massive AGB stars have shorter lifetimes. The He abundances of massive AGB stars are predicted to be quite high (e.g., Ventura & D’Antona 2009; Karakas 2010). Therefore, if 2G stars are formed from AGB ejecta earlier, then they can have high He abundances. Such 2G stars with high He abundances are likely to be formed in massive GCs where $f_{g,th}$ is lower, i.e., star formation can start earlier.

(5) SB and gravitational potentials of GC can combine to suppress the formation of massive and high-density gas clumps with $m_c \geq 8 M_\odot$, which implies that the formation of massive stars that can explode as SNII can be suppressed in GCs. This possible top-light IMF implies that the mass budget problem of GC formation is less severe than was suggested by previous theoretical models. Furthermore, such top-light IMF ensures that secondary star formation within GCs can last longer owing to the lack of energetic SNII of short-lived massive stars that can expel all of the remaining gas from GCs. It is suggested that young stellar objects within massive clusters with ages of several 10^7 yr can have the top-light IMF, if they exist in the clusters.

(6) The derived $f_{g,th}$ suggests that gas can be kept in the central regions of GCs without been converted into new stars for a significantly longer time scale. This can increase the probability that gas abundance in r -process elements ejected from neutron star merging can be trapped in GCs, because such trapping of high-speed ejecta requires high densities of intra-cluster gas (e.g., BT17). Therefore, $f_{g,th}$ can be closely related to the origin of abundances spreads in r -process elements in some GCs in the Galaxy.

(7) Thus, dense stellar systems such as GCs and stellar galactic nuclei can be a “double edge sword” for star formation within the systems. Deep gravitational potential well of such systems can retain gas ejected from existing stars such as AGB stars. Such retained gas can be used for secondary star formation within the systems. However, SB can suppress the mass growth of small gas clumps and thus secondary star formation within the systems, if the gas mass fractions are less than $f_{g,th}$ for star formation. This $f_{g,th}$ can result in discrete epochs of star formation, bursty nature of secondary star formation, retention of gas from merging of neutron stars and possibly from SNIa and delayed SNII in the early evolution of GCs.

6 ACKNOWLEDGMENT

I (Kenji Bekki; KB) am grateful to the referee for constructive and useful comments that improved this paper.

REFERENCES

- Adamo, A., et al., 2012, *MNRAS*, 426, 1185
 Armstrong, B., For, B.-Q., Bekki, K., 2018, *MNRAS*, 481, 3651
 Ashman, K. M., Zepf, S. E., 2001, *AJ*, 122, 1888
 Balin, J., 2018, *ApJ*, 863, 99 (B18)
 Bastian, N., Lardo, C., 2018, *ARA&A*, 56, 83
 Bate, M. R., Burkert, A., 1998, *MNRAS*, 288, 1060
 Bekki, K., 2006, *MNRAS*, 367L, 24
 Bekki, K., 2010, *ApJ*, 724, L99 (B10)
 Bekki, K., 2011, *MNRAS*, 412, 2241 (B11)
 Bekki, K., 2013, 432, 2298 (B13)
 Bekki, K., 2015, *MNRAS*, 449, 1625 (B15)
 Bekki, K., 2017a, *MNRAS*, 467, 1857 (B17a)
 Bekki, K., 2017b, *MNRAS*, 469, 2933 (B17b)
 Bekki, K., 2018 *A&A* in press (arXiv:1807.02309)
 Bekki, K., Norris, J. E., 2006, *ApJ*, 637, L109
 Bekki, K.; Campbell, S. W.; Lattanzio, J. C.; Norris, J. E., 2007, *MNRAS*, 377, 335
 Bekki, K., Chiba, M., 2007, *ApJ*, 665, 1164
 Bekki, K., Mackey, A. D., 2009, *MNRAS*, 394, 124
 Bekki, K., Yong, D., 2012, *MNRAS*, 419, 2063
 Bekki, K., Tsujimoto, T., 2016, *ApJ*, 831, 70
 Bekki, K., Tsujimoto, T., 2017, *ApJ*, 844, 34 (BT17)
 Bekki, K., Jerabkova, T., Kroupa, P., 2017, *MNRAS*, 471, 2242 (BJK17)
 Bianchini, P., et al., 2018, *MNRAS*, 481, 2125
 Binney, J., Tremaine, S., 1987 in *Galactic Dynamics*.
 Cabrera-Ziri, I., Bastian, N., Davies, B., Magris, G., Bruzual, G., Schweizer, F., 2014, *MNRAS*, 441, 2754
 Carretta, E., Bragaglia, A., Gratton, R. G., Lucatello, S., 2009, *A&A*, 505, 117
 Carretta, E., et al., 2014, *ApJL*, 795, 28
 Carretta, E., et al., 2015, *ApJ*, 810, 148
 Carretta, E., Bragaglia, A., Gratton, R. G., Lucatello, S., D’Orazi, V., 2012, *ApJ*, 750, L14
 Carretta, E., et al., 2018, *A&A*, 615, 17
 Conroy, C., Spergel, D. N., 2011, *ApJ*, 726, 36 (CS11)
 Da Costa, G. S., Held, E. V., Saviane, I., Gullieuszik, M., 2009, *ApJ*, 705, 1481
 Dale, J. E., Ngoumou, J., Ercolano, B., Bonnell, I. A., 2014, *MNRAS*, 442, 694
 D’Antona, F., Caloi, V., Montalbán, J., Ventura, P., Gratton, R., 2002, *A&A*, 395, 69
 D’Antona, F., Vesperini, E., D’Ercole, A., Ventura, P., Milone, A. P., Marino, A. F., Tailo, M., 2016, *MNRAS*, 458, 2122 (D16)
 D’Ercole, A., Vesperini, E., D’Antona, F., McMillan, S. L. W., & Recchi, S. 2008, *MNRAS*, 391, 825 (D08)
 D’Ercole, A., D’Antona, F., Vesperini, E., 2016, *MNRAS*, 461, 4088 (DDV16)
 Djorgovski, S. G., Gal, R. R., McCarthy, J. K., Cohen, J. G., de Carvalho, R. R., Meylan, G., Bendinelli, O., & Parmeggiani, G. 1997, *ApJL*, 474, 19
 Dominik et al. 2012, *ApJ*, 759, 52
 Elmegreen, B. G., 2017, *ApJ*, 836, 80
 For, B.Q., Bekki, K., 2017, *MNRAS*, 468, L11
 Fukui, Y., et al. 2015, *ApJL*, 807, 4
 Fukui, Y., et al. 2017, *PASJ*, L69, 5
 Fukui, Y., et al. 2018, *PASJ*, 70, 60
 Goldreich, P., Lynden-Bell, D., 1965, *MNRAS*, 130, 97
 Goudfrooij, P., et al., 2014, *ApJ*, 797, 35
 Gratton, R. G., Carretta, E., Bragaglia, A., 2012, *A&ARv*, 20, 50
 Greggio, L., Rensini, A., 2011, *Stellar populations. A User Guide from Low to High Redshift*
 Inoue, T., Fukui, Y., 2013, *ApJL*, 774, 31
 Johnson, C. I., et al. 2015, *AJ*, 150, 63
 Karakas, A. I., 2010, *MNRAS*, 403, 1413 (K10)
 Kim, J., Lee, Y.-W., 2018, *ApJ* in press (arXiv:1807.01317)
 Klessen, Ralf S.; Burkert, Andreas; Bate, M. R., 1998, *ApJL*, 501, 205
 Kroupa, P., et al., 2013, *Springer Science+Business Media Dordrecht*, 115
 Lardo, C., et al. 2013, *MNRAS*, 433, 1941
 Leigh, N. W. C., Boker, T., Maccarone, T. J., Perets, H. B., 2013, 429, 2997 (L13)
 Marino, A. F., Milone, A. P., Piotto, G., Villanova, S., Bedin, L. R., Bellini, A., Renzini, A., 2009, *A&A*, 505, 1099
 Marino, A. F., et al. 2011, *A&A*, 532, 8
 Marino, A. F. et al. 2015, *MNRAS*, 450, 815
 Marino, A. F. et al. 2018, *ApJ*, 859, 81
 Mastrobuono-Battisti, A., Perets, H. B., 2013, *ApJ*, 779, 85
 Maxwell, A. J., Wadsley, J. Couchman, H. M. P.; Sills, A., 2014, *MNRAS*, 439, 2043
 McKenzie, M., Bekki, K., 2018, *MNRAS*, 479, 3126
 Meyers, P. C., 1978, *ApJ*, 225, 380
 Milone, A. P., et al. 2013, *A&A*, 555, 143
 Milone, A. P., et al. 2017, *MNRAS*, 464, 3636
 Milone, A. P., Marino, A. F., Mastrobuono-Battisti, A., Lagioia, E. P., 2018a, *MNRAS*, 479, 5005
 Milone, A. P., et al. 2018b, *MNRAS*, 481, 5098
 Navarro, J. F., Frenk, C. S., White, S. D. M., 1996, *ApJ*, 462, 563 (NFW)
 Nelson, A. F., 2006, *MNRAS*, 373, 1039
 Neto, A. F., et al., 2007, *MNRAS*, 381, 1450
 Niederhofer, F., et al., 2016, *MNRAS* in press (arXiv:1612.00400)
 Pflamm-Altenburg, J., Kroupa, P., 2009, *MNRAS*, 397, 488
 Phillips, J. P., 1999, *A&AS*, 134, 241
 Piotto, G., et al., 2005, 621, 777
 Prantzos, N., Charbonnel, C., 2006, *A&A*, 458, 135
 Renzini, A., et al., 2015, *MNRAS*, 454, 4197
 Roederer, I. U., 2011, *ApJ*, 732, L17
 Saigo, K., Matsumoto, T., Hanawa, T., 2000, *ApJ*, 531, 971
 Sneden, C., Kraft, R. P., Shetrone, M. D., Smith, G. H., Langer, G. E., & Prosser, C. F. 1997, *AJ*, 114, 1964
 Sobeck et al. 2011, *AJ*, 141, 175
 Tailo, M., et al. 2015, *Nature*, 523, 318 (T15)
 Truelove, J. K., Klein, R. I., McKee, C. F., Holliman, J. H. II., Howell, L. H., Greenough, J. A., 1997, *ApJL*, 489, 179
 Ventura, P.; D’Antona, F., 2009, *A&A*, 499, 835
 Vesperini, E., Hong, J., Webb, J. J., D’Antona, F., D’Ercole, A., 2018, *MNRAS*, 476, 2731
 Worley, C. C., Hill, V., Sobeck, J., & Carretta, E. 2013, *A&A*, 553, 47

Yong, D., Roederer, I. U., Grundahl, F., Da Costa, G. S., Karakas, A. I., Norris, J. E., Aoki, W., Fishlock, C. K., Marino, A. F., Milone, A. P., & Shingles, L. J. 2014, MNRAS, 441, 3396

Zaprtas, E., et al. 2017, A&A, 601, 29